Paper BIII: Diatomic Molecules & Laser Physics

Prof. Simon Hooker

Michaelmas Term 2012

Contents

Lecture 1

Introduction to Molecules and the Born–Oppenheimer Approximation

1.1 Introduction

In these 8 lectures we will look at the physics of diatomic molecules and of laser systems. I would be very grateful if any errors or unclear passages could be brought to my attention (email: simon.hooker@physics.ox.ac.uk).

1.1.1 Recommended books on diatomic molecules

- H. Haken and H. C. Wolf, 'Molecular Physics and Elements of Quantum Chemistry.' Covers our syllabus, and much else besides.
- J. M. Brown, 'Molecular Spectroscopy.' A useful brief introduction.
- Bransden & Joachain, 'Physics of Atoms and Molecules.' Well beyond the level required. Chapters 10 and 11 (particularly sections 10.1 - 10.4, and 11.1 - 11.3) contain useful information for this course.

1.1.2 Recommended books on laser physics

- S. M. Hooker & C. E. Webb, 'Laser Physics,' Oxford University Press (2010). You can make up your own mind about this ...
- C.C. Davies, 'Lasers and Electro-Optics: Fundamentals and Engineering,' Cambridge University Press (1996). Very readable, clear diagrams, excellent coverage of nearly all of the course material at about the right level.
- O. Svelto, 'Principles of Lasers,' Plenum Press, Fourth Edition (1998). Readable, good coverage of material at about the right level.

1.1.3 Initial observations

A diatomic molecule is formed from two atoms or ions. As we bring two atoms or ions closer together, the electrons in closed shells will usually remain in closed shells and we therefore only need worry about the valence electrons. At separations characteristic of a molecule, the valance electrons are often no longer uniquely associated with one atom or the other, and instead are distributed throughout the molecule. The distribution of the electrons within the molecule will determine whether or not the molecule remains bound and, if so, the characteristics of the molecular state; these include, the equilibrium separation of the constituent atoms, the absorption frequencies, and the energy required to dissociate the molecule.

1.1.4 Orders of magnitude

We will need to consider the following interactions:

- Electron-nuclear interaction:

$$-\frac{Z_A e^2}{4\pi\epsilon_0 \left|\boldsymbol{r}-\boldsymbol{R_A}\right|}$$

- Electron-electron interaction:

$$\frac{e^2}{4\pi\epsilon_0\,|\boldsymbol{r_1}-\boldsymbol{r_2}|}$$

- Nuclear-nuclear interaction:

$$\frac{Z_A Z_B e^2}{4\pi\epsilon_0\,|\boldsymbol{R_A}-\boldsymbol{R_B}|}$$

Since the nuclear-nuclear, electron-nuclear and electron-electron separations are similar, the interactions above have approximately the same magnitude. Hence the forces between electrons and nuclei are also similar. However, since the masses of the nuclei are much greater than the electron mass, the *velocities of the nuclei are much lower than those of electrons.* This fact will lead to a great simplification, known as the **Born-Oppenheimer approximtion**.

Electronic energy

Suppose that the valence electrons of the molecule are confined to a region of size a. From the Uncertainty Principle,

$$\Delta p \approx \frac{\hbar}{a}. \tag{1.1}$$

Since the mean momentum must be zero, we have,

$$p^2 \approx \left(\frac{\hbar}{a}\right)^2. \tag{1.2}$$

We expect the electronic energy of the molecule, E_e, to be of the order of the kinetic energy of the electrons and hence,

$$E_\mathrm{e} \approx \frac{p^2}{2m} = \frac{\hbar^2}{2ma^2}. \tag{1.3}$$

If we take $a \approx 2a_0 \approx 1\times10^{-10}\,\mathrm{m}$, we find $E_\mathrm{e} \approx 4\,\mathrm{eV} \approx 30,000\,\mathrm{cm}^{-1}$. Hence we expect the electronic levels of molecules to have energies of several eV, or tens of thousands of wavenumbers (in units of cm^{-1}), just as in atoms.

The *timescale* of the electronic motion can be estimated as h/E_e, which is of order 1 fs.

Vibrational energy

The potential energy of vibrational motion has the form,

$$U(x) = (1/2)\mu\omega_\mathrm{v}^2 x^2, \tag{1.4}$$

where $\mu = M_A M_B/(M_A+M_B)$ is the **reduced nuclear mass** (we will return to this). Now, the molecule will dissociate for extensions of order a, i.e. $U(a) \approx E_\mathrm{e}$. Hence,

$$\begin{aligned} U(a) &\approx E_\mathrm{e} \\ \Rightarrow \frac{1}{2}\mu\omega_\mathrm{v}^2 a^2 &\approx \frac{\hbar^2}{2ma^2} \\ \Rightarrow \omega_\mathrm{v} &\approx \sqrt{\frac{\hbar^2}{\mu m a^4}}. \end{aligned}$$

We then find,

$$E_\mathrm{v} \approx \hbar\omega_\mathrm{v} \approx \sqrt{\frac{m}{\mu}}E_\mathrm{e}. \tag{1.5}$$

Hence we conclude that vibrational energies are smaller than the electronic energy by a factor of order $\sqrt{m/\mu}$, i.e. about a factor of 100 smaller.

Motion	Energy	Energy (cm^{-1})	Period	Spectral region
Electronic	10 eVs	50,000	1 fs	visible - ultraviolet
Vibrational	100 meV	1000	100 fs	infra-red
Rotational	1 meV	10	10 ps	far infra-red & microwave

Table 1.1: Orders of magnitude of the energies and time-scales of the electronic, vibrational, and rotational motion of diatomic molecules.

Rotational energy

To estimate the energy associated with rotational motion we note that the angular momentum of the rotating molecule is expected to be of order $\hbar$. Hence $L = I\omega_{\rm r} \approx \hbar$, where $I = \mu a^2$ is the moment of inertia for rotation about an axis passing through the centre of mass and perpendicular to the inter-nuclear axis. Hence,

$$I\omega_{\rm r} = \mu a^2 \omega_{\rm r} \approx \hbar$$
$$\Rightarrow \omega_{\rm r} \approx \frac{\hbar}{I} = \frac{\hbar}{\mu a^2}$$

From this we deduce that the rotational energy is given by,

$$E_{\rm r} = \frac{1}{2} I \omega_{\rm r}^2 = \frac{\hbar^2}{2I} = \frac{\hbar^2}{\mu a^2} \approx \frac{m}{\mu} E_{\rm e}, \tag{1.6}$$

i.e. another factor $\sqrt{m/\mu}$ smaller than the vibrational energy.

Hence, to summarize this section:

$$E_{\rm e} \gg E_{\rm v} \gg E_{\rm r}$$
$$T_{\rm e} \ll T_{\rm v} \ll T_{\rm r}$$

Table 1.1 presents typical values for the energies and timescales associated with the electronic, vibrational, and rotational motion of diatomic molecules.

1.2 The molecular hydrogen ion

In order to develop a more quantitative understanding we will consider the simplest possible diatomic molecule: the molecular hydrogen ion, comprising a pair of protons and a *single* electron. The co-ordinate system we will use is illustrated in Fig. 1.1.

We will simplify things even further by considering the nuclei to be fixed in space. As such we will only investigate the motion of the electrons in the fields of the nuclei, and we will ignore the vibrational and rotational motion of the nuclei.

The Hamiltonian of the system is:

$$\hat{\mathcal{H}} = -\frac{\hbar^2}{2m}\nabla_r^2 - \frac{e^2}{4\pi\epsilon_0 \left|\boldsymbol{r} - \boldsymbol{R_A}\right|} - \frac{e^2}{4\pi\epsilon_0 \left|\boldsymbol{r} - \boldsymbol{R_B}\right|} + \frac{e^2}{4\pi\epsilon_0 \left|R\right|}, \tag{1.7}$$

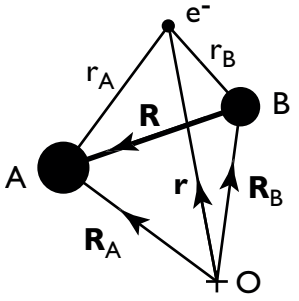

Figure 1.1: Co-ordinate system used to solve the Schrödinger equation for the molecular hydrogen ion

where $\boldsymbol{R} = \boldsymbol{R_A} - \boldsymbol{R_B}$.

Unusually for diatomic molecules this can be solved exactly (using confocal elliptic coordinates[1]). However it is more instructive to use a variational method since this is also used to solve more complicated molecules.

We wish to solve,

$$\hat{\mathcal{H}}\psi(\boldsymbol{R}_A, \boldsymbol{R}_B, \boldsymbol{r}) = E(R)\psi(\boldsymbol{R}_A, \boldsymbol{R}_B, \boldsymbol{r}). \tag{1.8}$$

At large internuclear separation R we expect that the electron will be associated with one nucleus or the other. Hence

$$\psi(\boldsymbol{R}_A, \boldsymbol{R}_B, \boldsymbol{r}) \to \phi_{1s}(\boldsymbol{r} - \boldsymbol{R}_A) \equiv \phi_{1s}(\boldsymbol{r}_A) \qquad \text{or} \qquad \psi(\boldsymbol{R}_A, \boldsymbol{R}_B, \boldsymbol{r}) \to \phi_{1s}(\boldsymbol{r} - \boldsymbol{R}_B) \equiv \phi_{1s}(\boldsymbol{r}_B), \tag{1.9}$$

where we have introduced the notation $\boldsymbol{r} - \boldsymbol{R}_A \equiv \boldsymbol{r}_A$. It is clear that the two limiting wave functions above are degenerate in energy.

We also note that inversion of the *electron* coordinates through the centre of mass (i.e. the midpoint of the internuclear axis) leaves the Hamiltonian unchanged. This fact, and eqn (1.9) suggest that we form even (known as **"gerade"**) and odd (known as **"ungerade"**) combinations of the two single-atom wave functions:

$$\psi_{\mathrm{g,u}}(\boldsymbol{R}_A, \boldsymbol{R}_B, \boldsymbol{r}) = \phi_{1s}(\boldsymbol{r} - \boldsymbol{R}_A) \pm \phi_{1s}(\boldsymbol{r} - \boldsymbol{R}_B). \tag{1.10}$$

These combinations, $\psi_{\mathrm{g,u}}(\boldsymbol{R}, \boldsymbol{r})$, are not exact solutions of the Schrödinger equation, but they are sensible trial wave functions which behave correctly in the limit of large internuclear separation and, as required, have a definite inversion symmetry for all R.

We can now evaluate the energy,

$$E(R) < \frac{\langle\psi|\,\hat{\mathcal{H}}\,|\psi\rangle}{\langle\psi|\,\psi\rangle}. \tag{1.11}$$

By the Ritz variational principle the ground state energy must be less than or equal to this value. Since the wave functions $\phi_{1s}(\boldsymbol{r} - \boldsymbol{R}_A)$ and $\phi_{1s}(\boldsymbol{r} - \boldsymbol{R}_B)$ are known, then eqn (1.11) can be evaluated to give an upper bound for the ground-state electronic energy as a function of the internuclear separation R. In practice the required integrals are cumbersome, so here we will outline the key steps and draw some general solutions from the results.

1.2.1 Evaluating $E(R)$

The denominator

Considering first the denominator, which we will call D, on substituting for $\psi_{\mathrm{g,u}}$ we find,

$$\begin{aligned} D &= \langle\phi_{1s}(\boldsymbol{r}_A) \pm \phi_{1s}(\boldsymbol{r}_B)\,|\phi_{1s}(\boldsymbol{r}_A) \pm \phi_{1s}(\boldsymbol{r}_B)\rangle \\ &= \langle\phi_{1s}(\boldsymbol{r}_A)\,|\phi_{1s}(\boldsymbol{r}_A)\rangle + \langle\phi_{1s}(\boldsymbol{r}_B)\,|\phi_{1s}(\boldsymbol{r}_B)\rangle \pm \langle\phi_{1s}(\boldsymbol{r}_A)\,|\phi_{1s}(\boldsymbol{r}_B)\rangle \pm \langle\phi_{1s}(\boldsymbol{r}_B)\,|\phi_{1s}(\boldsymbol{r}_A)\rangle\,. \end{aligned}$$

Now,

$$\langle\phi_{1s}(\boldsymbol{r}_A)\,|\phi_{1s}(\boldsymbol{r}_A)\rangle = \langle\phi_{1s}(\boldsymbol{r}_B)\,|\phi_{1s}(\boldsymbol{r}_B)\rangle = 1 \tag{1.12}$$

and we define,

$$\mathcal{I}(R) = \langle\phi_{1s}(\boldsymbol{r}_A)\,|\phi_{1s}(\boldsymbol{r}_B)\rangle = \left(\langle\phi_{1s}(\boldsymbol{r}_B)\,|\phi_{1s}(\boldsymbol{r}_A)\rangle\right)^*. \tag{1.13}$$

We may then write the denominator in the form:

$$D = 2\left[1 \pm \Re\left[\mathcal{I}(R)\right]\right]. \tag{1.14}$$

[1] If you are interested, see Bransden and Joachain

The numerator

Substituting for $\psi_{\mathrm{g,u}}(\boldsymbol{R},\boldsymbol{r})$ we find that the **numerator** becomes,

$$\langle\phi_{1s}(\boldsymbol{r}_A)\pm\phi_{1s}(\boldsymbol{r}_B)|\,\hat{\mathcal{H}}\,|\phi_{1s}(\boldsymbol{r}_A)\pm\phi_{1s}(\boldsymbol{r}_B)\rangle = \mathcal{H}_{AA}+\mathcal{H}_{BB}\pm\mathcal{H}_{AB}\pm\mathcal{H}_{BA} \tag{1.15}$$

$$= 2\left[\mathcal{H}_{AA}\pm\Re\left(\mathcal{H}_{AB}\right)\right], \tag{1.16}$$

which follows since $\mathcal{H}_{AA}=\mathcal{H}_{BB}$ and $\mathcal{H}_{AB}=\mathcal{H}^*_{BA}$.

Hence we have,

$$E(R)\leq\frac{\mathcal{H}_{AA}\pm\Re\left(\mathcal{H}_{AB}\right)}{1\pm\Re\left[\mathcal{I}(R)\right]}. \tag{1.17}$$

Evaluation of integrals

Let us first evaluate H_{AA} and H_{AB}. To do this we note that,

$$\hat{\mathcal{H}}\phi_{1s}(\boldsymbol{r}_A)=\left\{-\frac{\hbar^2}{2m}\nabla^2_{\boldsymbol{r}}-\frac{e^2}{4\pi\epsilon_0\left|\boldsymbol{r}-\boldsymbol{R}_A\right|}\right\}\phi_{1s}(\boldsymbol{r}_A)+\left[-\frac{e^2}{4\pi\epsilon_0\left|\boldsymbol{r}-\boldsymbol{R}_B\right|}+\frac{e^2}{4\pi\epsilon_0 R}\right]\phi_{1s}(\boldsymbol{r}_A). \tag{1.18}$$

Now, the term in curly brackets is the Hamiltonian for a hydrogen *atom* formed by the electron orbiting nucleus A. Consequently we may write,

$$\hat{\mathcal{H}}\phi_{1s}(\boldsymbol{r}_A)=E_{1s}\phi_{1s}(\boldsymbol{r}_A)+\left[-\frac{e^2}{4\pi\epsilon_0\left|\boldsymbol{r}-\boldsymbol{R}_B\right|}+\frac{e^2}{4\pi\epsilon_0 R}\right]\phi_{1s}(\boldsymbol{r}_A), \tag{1.19}$$

where E_{1s} is the ground-state energy of the hydrogen *atom*. Hence we have,

$$\mathcal{H}_{AA}=E_{1s}+\langle\phi_{1s}(\boldsymbol{r}_A)|-\frac{e^2}{4\pi\epsilon_0\left|\boldsymbol{r}-\boldsymbol{R}_B\right|}+\frac{e^2}{4\pi\epsilon_0 R}\,|\phi_{1s}(\boldsymbol{r}_A)\rangle \tag{1.20}$$

$$=E_{1s}+\frac{e^2}{4\pi\epsilon_0 R}+\mathcal{J}(R), \tag{1.21}$$

where,

$$\mathcal{J}(R)=-\int\phi_{1s}(\boldsymbol{r}_A)^*\frac{e^2}{4\pi\epsilon_0\left|\boldsymbol{r}-\boldsymbol{R}_B\right|}\phi_{1s}(\boldsymbol{r}_A)\mathrm{d}\boldsymbol{r} \tag{1.22}$$

$$=\int(-e)\left|\phi_{1s}(\boldsymbol{r}_A)\right|^2\frac{e}{4\pi\epsilon_0\boldsymbol{r}_B}\mathrm{d}\boldsymbol{r} \tag{1.23}$$

$$=\int\rho(\boldsymbol{r}_A)\frac{e}{4\pi\epsilon_0\boldsymbol{r}_B}\mathrm{d}\boldsymbol{r}. \tag{1.24}$$

The integral $\mathcal{J}$ is known as the **direct integral**. Since $\rho(\boldsymbol{r}_A)=(-e)\left|\phi_{1s}(\boldsymbol{r}_A)\right|^2$ is the charge density of a 1s electron associated with nucleus A, we can see that the direct integral is simply the energy of the electrostatic interaction between nucleus B and the hydrogen atom formed by a 1s electron orbiting nucleus A.

To evaluate $\mathcal{H}_{AB}$ we note that form eqn (1.19),

$$H\phi_{1s}(\boldsymbol{r}_B)=E_{1s}\phi_{1s}(\boldsymbol{r}_B)+\left[-\frac{e^2}{4\pi\epsilon_0\left|\boldsymbol{r}-\boldsymbol{R}_A\right|}+\frac{e^2}{4\pi\epsilon_0 R}\right]\phi_{1s}(\boldsymbol{r}_B). \tag{1.25}$$

Hence,

$$H_{AB}=\langle\phi_{1s}(\boldsymbol{r}_A)|\,E_{1s}+\frac{e^2}{4\pi\epsilon_0 R}\,|\phi_{1s}(\boldsymbol{r}_B)\rangle+\mathcal{K}(R).$$

where,

$$\mathcal{K}(R)=-\langle\phi_{1s}(\boldsymbol{r}_A)|\,\frac{e^2}{4\pi\epsilon_0 r_A}\,|\phi_{1s}(\boldsymbol{r}_B)\rangle=\int\left[-e\phi_{1s}(\boldsymbol{r}_A)^*\phi_{1s}(\boldsymbol{r}_B)\right]\frac{e}{4\pi\epsilon_0 r_A}\mathrm{d}\boldsymbol{r}. \tag{1.26}$$

This is an **exchange integral** and it has no classical analogue. Note however, that the direct and exchange integrals which appear in this treatment of the hydrogen ion *are* analogous to the direct and exchange integrals arising in the treatment of the helium atom.

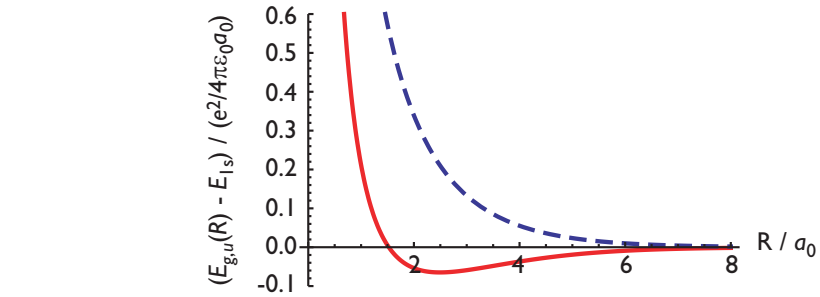

(a)

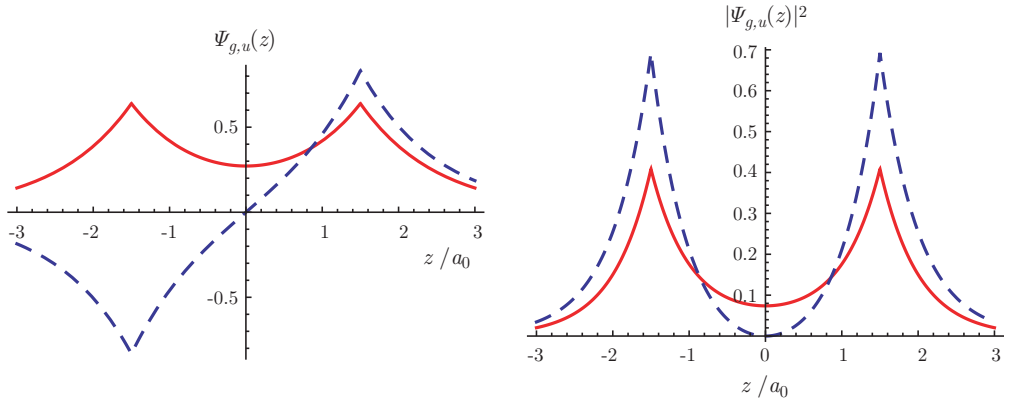

(b)

Figure 1.2: Calculated energy curves and wave functions for the H_2^+ ion. (a) Energy curves $E_{\rm g,u}(R)$ calculated from eqn (1.29). (b) The wave functions $\psi_{\rm g,u}(z)$ and $|\psi_{\rm g,u}(z)|^2$ plotted as a function of the distance z along the nuclear axis for an internuclear separation $R = 3a_0$, where a_0 is the Bohr radius.

Form of potential energy curve

The integrals $\mathcal{I}(R)$, $\mathcal{J}(R)$, and $\mathcal{K}(R)$ can be evaluated upon substitution of the hydrogenic wave functions:

$$\phi_{1s}(\boldsymbol{r}_A) = \left(\frac{1}{\pi a_0^3}\right)^{1/2} \exp(-r_A/a_0). \tag{1.27}$$

On doing this, and evaluating some tricky integrals, it is found that

$$E_{\rm g,u}(R) \leq E_{1s} + \frac{e^2}{4\pi\epsilon_0 R} + \frac{\mathcal{J}(R) \pm \mathcal{K}(R)}{1 \pm \mathcal{I}(R)} \tag{1.28}$$

$$\leq E_{1s} + \frac{e^2}{4\pi\epsilon_0 R} \frac{(1+R')\exp(-2R') \pm \left(1 - \frac{2}{3}R'^2\right)\exp(-R')}{1 \pm \left(1 + R' + \frac{1}{3}R'^2\right)\exp(-R')} \tag{1.29}$$

where $R' = R/a_0$. Figure 1.2(a) shows $E_{\rm g,u}(R)$ as a function of the internuclear separation R. We note several key features:

- At large R both curves tend to E_{1s}, the energy of a H atom in the ground state
- The even-parity state ('g') exhibits a minimum, i.e. it is bound. The corresponding wave function is known as a **bonding orbital**.
- The odd-parity state does not possess a minimum, and forms instead a repulsive curve. The associated wave function is an **anti-bonding orbital**. An H_2^+ molecule in this state will rapidly dissociate, converting the potential energy $E(R)$ to kinetic energy of the constituents; at large R these will be a hydrogen atom and a proton.

The differences in the potential curves may be understood by considering the form of the wave functions $\psi_{\rm g,u}(z)$, which are plotted in Fig. 1.2(b). We see that $\psi_{\rm g}$ has a larger amplitude in the region between the

two nuclei and hence an electron in this state has a relatively high probability of being between the nuclei. When it is between the nuclei the electron interacts strongly with *both* nuclei, leading to strong binding. In contrast, an electron in ψ_u has a distinctly lower probability of being between the nuclei — partly because the wave function has a node at the centre of mass — and as a consequence we expect that the average potential energy of electrons in this state will be less negative than for the gerade state.

This is the usual explanation given to explain the difference in energies between the two states. However, other effects can play a role. In particular the spatial extent of the wave functions can differ; this means that the kinetic energy of the state will be different, since the kinetic energy operator depends on the spatial derivatives of the wave function. When deciding which states are more strongly bound, differences in both the kinetic and potential energies of the states must be accounted for.[2]

[2]For details, see section 8.2, Atkins & Friedman, 'Molecular Quantum Mechanics' OUP.

Lecture 2

The Born–Oppenheimer Approximation

2.1 The Born-Oppenheimer approximation

Neglecting spin-orbit, spin-spin interactions etc, the Hamiltonian of a diatomic molecule can be written as,

$$\hat{\mathcal{H}} = \hat{T}_\mathrm{n} + \hat{T}_\mathrm{e} + V, \tag{2.1}$$

where $\hat{T}_\mathrm{n}$ is the kinetic energy of the nuclei, $\hat{T}_\mathrm{e}$ the kinetic energy of the electrons, V is the potential energy. Writing these out:

$$\begin{aligned}
\hat{T}_\mathrm{n} &= -\frac{\hbar^2}{2M_1}\nabla^2_{\boldsymbol{R_A}} - \frac{\hbar^2}{2M_2}\nabla^2_{\boldsymbol{R_B}} && \text{KE of nuclei} \\
\hat{T}_\mathrm{e} &= \sum_i -\frac{\hbar^2}{2m_i}\nabla^2_{\boldsymbol{r_i}} && \text{KE of electrons} \\
V &= \sum_i -\frac{Z_1 e^2}{4\pi\epsilon_0\,|\boldsymbol{r_i} - \boldsymbol{R_A}|} - \frac{Z_2 e^2}{4\pi\epsilon_0\,|\boldsymbol{r_i} - \boldsymbol{R_B}|} && \text{electron-nuclear interaction} \\
&+ \sum_i \sum_{j>i} \frac{e^2}{4\pi\epsilon_0\,|\boldsymbol{r_i} - \boldsymbol{r_j}|} && \text{electron-electron repulsion} \\
&+ \frac{Z_1 Z_2 e^2}{4\pi\epsilon_0\,|\boldsymbol{R_A} - \boldsymbol{R_B}|} && \text{nuclear repulsion.}
\end{aligned}$$

In the above equations the origin of co-ordinates is fixed in the laboratory, as shown in Fig. 2.1(a). If we move the origin to the centre of mass of the two nuclei then the operator $\hat{T}_\mathrm{n}$ becomes,

$$\hat{T}_\mathrm{n} = -\frac{\hbar^2}{2\mu}\nabla^2_{\boldsymbol{R}}, \tag{2.2}$$

where $\boldsymbol{R} = \boldsymbol{R_A} - \boldsymbol{R_B}$, and the reduced mass is given by,

$$\frac{1}{\mu} = \frac{1}{M_A} + \frac{1}{M_B}. \tag{2.3}$$

Note that now $\hat{T}_\mathrm{n}$ is simply the kinetic energy operator of a *single particle*, of mass μ, with a position vector $\boldsymbol{R}$.[1] Figure 2.1 shows the relation between the COM and lab co-ordinate systems.

We wish to solve the Schrödinger equation,

$$\hat{\mathcal{H}}\Psi(\boldsymbol{R}, \boldsymbol{r_1}, \boldsymbol{r_2}, \ldots \boldsymbol{r_N}) = E\Psi(\boldsymbol{R}, \boldsymbol{r_1}, \boldsymbol{r_2}, \ldots). \tag{2.4}$$

[1] We have ignored the mass of the electrons, which will be small compared to μ. We have also ignored the motion of the centre of mass; including this leads to multiplication of the molecular wave function by a term of the form $\exp(i\boldsymbol{K}\cdot\boldsymbol{R}_s)$ where $\hbar\boldsymbol{K}$ and $\boldsymbol{R}_s$ are the momentum and position of the centre of mass. For further details see Haken & Wolf, section 11.1.1 or Bransden & Joachain section 10.2

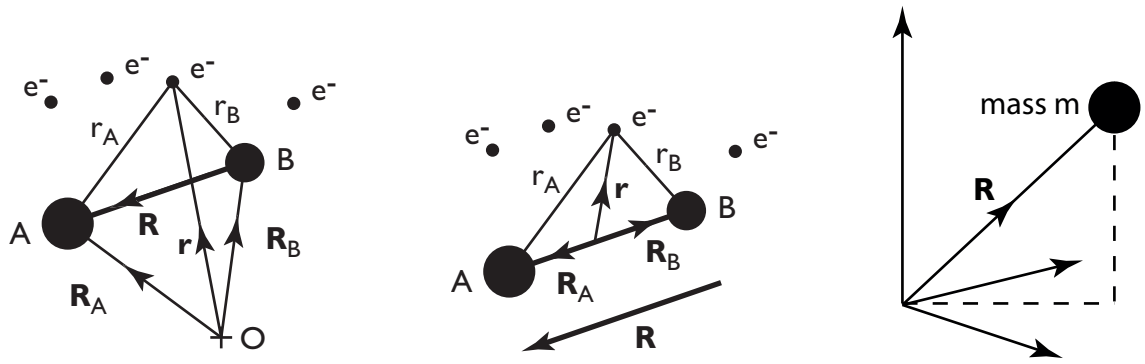

Figure 2.1: Co-ordinate systems. (a) the lab co-ordinate system; (b) the centre of mass co-ordinate system; (c) co-ordinates of a single particle of mass μ.

For convenience we will introduce the shorthand $\boldsymbol{r} \equiv \boldsymbol{r_1}, \boldsymbol{r_2}, \ldots \boldsymbol{r_N}$, so that the molecular wave function may be written as $\Psi(\boldsymbol{R}, \boldsymbol{r})$.

First we remind ourselves of the Schrödinger equation for *fixed nuclei*:

$$\hat{\mathcal{H}}_\mathrm{e}\psi_\mathrm{e}(\boldsymbol{R}, \boldsymbol{r}) = \left[\hat{T}_\mathrm{e} + V(\boldsymbol{R}, \boldsymbol{r})\right] \psi_\mathrm{e}(\boldsymbol{R}, \boldsymbol{r}) = E_\mathrm{e}(R)\psi_\mathrm{e}(\boldsymbol{R}, \boldsymbol{r}), \tag{2.5}$$

where $\hat{\mathcal{H}}_\mathrm{e}$ is the Hamiltonian for fixed nuclei.

The electrons move much faster than the nuclei and hence they can follow, essentially instantaneously, the nuclei as they move. We will therefore attempt to find solutions which may be written in the form,

$$\Psi(\boldsymbol{R}, \boldsymbol{r}) = \psi_\mathrm{n}(\boldsymbol{R})\psi_\mathrm{e}(\boldsymbol{R}, \boldsymbol{r}),$$

i.e. a product of a nuclear wave function $\psi_\mathrm{n}(\boldsymbol{R})$ and the electronic wave function $\psi_\mathrm{e}(\boldsymbol{R}, \boldsymbol{r})$. We now make the **Born–Oppenheimer approximation** and assume that electronic wave function depends only very weakly on the internuclear separation $\boldsymbol{R} = \boldsymbol{R_A} - \boldsymbol{R_B}$. If we ignore the dependence of $\psi_\mathrm{e}(\boldsymbol{R}, \boldsymbol{r})$ on $\boldsymbol{R}$ the Schrödinger equation then simplifies to:[2]

$$\left[\hat{T}_\mathrm{n} + \hat{T}_\mathrm{e} + V\right] \psi_\mathrm{n}(\boldsymbol{R})\psi_\mathrm{e}(\boldsymbol{R}, \boldsymbol{r}) = E\psi_\mathrm{n}(\boldsymbol{R})\psi_\mathrm{e}(\boldsymbol{R}, \boldsymbol{r}) \tag{2.6}$$

$$\Rightarrow \psi_\mathrm{e}\hat{T}_\mathrm{n}\psi_\mathrm{n} + \psi_\mathrm{n}\left[\hat{T}_\mathrm{e} + V\right] \psi_\mathrm{e} = E\psi_\mathrm{n}\psi_\mathrm{e} \tag{2.7}$$

$$\Rightarrow \frac{1}{\psi_\mathrm{n}}\hat{T}_\mathrm{n}\psi_\mathrm{n} + \left\{\frac{1}{\psi_\mathrm{e}}\left[\hat{T}_\mathrm{e} + V\right] \psi_\mathrm{e}\right\} = E \tag{2.8}$$

From the Schrödinger equation for fixed nuclei, we see that the term in curly brackets is equal to $E_\mathrm{e}(R)$, and hence eqn (2.8) becomes,

$$\left[\hat{T}_\mathrm{n} + E_\mathrm{e}(R)\right] \psi_\mathrm{n} = E\psi_\mathrm{n}. \tag{2.9}$$

To summarize, we have reduced the problem to two Schrödinger equations:

$$\hat{\mathcal{H}}_\mathrm{e}\psi_\mathrm{e}(\boldsymbol{R}, \boldsymbol{r}) = E_\mathrm{e}(R)\psi_\mathrm{e}(\boldsymbol{R}, \boldsymbol{r}). \qquad \text{electronic wave equation} \tag{2.10}$$

$$\left[\hat{T}_\mathrm{n} + E_\mathrm{e}(R)\right] \psi_\mathrm{n}(\boldsymbol{R}) = E\psi_\mathrm{n}(\boldsymbol{R}). \qquad \text{nuclear wave equation} \tag{2.11}$$

Within the Born–Oppenheimer approximation, therefore, the energy levels and wave functions of the molecule may be found (at least in principle) as follows:

- The Schrödinger equation for electrons moving in the field of the *fixed nuclei* is solved, yielding the **electronic energy** $E_\mathrm{e}(R)$. Notice that the electronic energy can only depend on the *magnitude* of the nuclear separation, R. The **electronic wave function** $\psi_\mathrm{e}(\boldsymbol{R}, \boldsymbol{r})$ will also depend on the *orientation* of $\boldsymbol{R}$ through a straightforward rotation of coordinate system.
- The total energy of the molecule E is found by solving the Schrödinger equation for the nuclei moving in the potential $E_\mathrm{e}(R)$. Solution to this problem will yield the **nuclear wave function** $\psi_\mathrm{n}(\boldsymbol{R})$.

[2] See Haken & Wolf section 11.1 for a demonstration that the neglected terms are indeed usually small.

2.1.1 Solution of the nuclear wave equation

As we have seen, the electronic energy $E_\mathrm{e}(R)$ acts as potential in which the nuclei (represented by a single particle of mass μ) move. The potential is spherically symmetric and hence, just as for atoms, we write:

$$\psi_\mathrm{n}(\boldsymbol{R}) = \psi'_\mathrm{v}(R)\psi_\mathrm{r}(\Theta,\Phi). \tag{2.12}$$

This gives the usual separation into an angular equation and a **radial equation**,

$$\left[-\frac{\hbar^2}{2\mu}\frac{1}{R^2}\frac{\partial}{\partial R}\left(R^2\frac{\partial}{\partial R}\right) + \frac{J(J+1)\hbar^2}{2\mu R^2} + E_\mathrm{e}(R)\right]\psi'_\mathrm{v}(R) = E\psi'_\mathrm{v}(R) \tag{2.13}$$

where $J(J+1)\hbar^2$ is the angular momentum of the nuclei rotating about the centre of mass.

As in atomic physics we can write a *reduced* radial wave function,

$$\psi_\mathrm{v}(R) = R\psi'_\mathrm{v}(R), \tag{2.14}$$

so that the radial equation becomes,

$$\left[-\frac{\hbar^2}{2\mu}\frac{\mathrm{d}^2}{\mathrm{d}R^2} + \frac{J(J+1)\hbar^2}{2\mu R^2} + E_\mathrm{e}(R)\right]\psi_\mathrm{v}(R) = E\psi_\mathrm{v}(R) \tag{2.15}$$

$$\Rightarrow \left[-\frac{\hbar^2}{2\mu}\frac{\mathrm{d}^2}{\mathrm{d}R^2} + V_\mathrm{eff}(R)\right]\psi_\mathrm{v}(R) = E\psi_\mathrm{v}(R) \tag{2.16}$$

This is a simple, *one-dimensional* Schrödinger equation for a particle of mass μ moving in an effective potential,

$$V_\mathrm{eff} = E_\mathrm{e}(R) + \frac{J(J+1)\hbar^2}{2\mu R^2}. \tag{2.17}$$

Approximations for V_eff

For any *bound* state we can expand $E_\mathrm{e}(R)$:

$$E_\mathrm{e}(R) = E_\mathrm{e}(R_0) + \left.\frac{\mathrm{d}E_\mathrm{e}}{\mathrm{d}R}\right|_{R_0}(R-R_0) + \frac{1}{2}\left.\frac{\mathrm{d}^2E_\mathrm{e}}{\mathrm{d}R^2}\right|_{R_0}(R-R_0)^2 + \ldots \tag{2.18}$$

The second term must be zero since by definition the potential has a minimum at $R = R_0$, and hence

$$E_\mathrm{e}(R) \approx E_\mathrm{e}(R_0) + \frac{1}{2}K\left(R-R_0\right)^2, \tag{2.19}$$

where K is the spring constant of the bond.

We can also approximate the centrifugal repulsion term by its value at the equilibrium separation R_0:

$$\frac{J(J+1)\hbar^2}{2\mu R^2} \approx \frac{J(J+1)\hbar^2}{2\mu R_0^2} = \frac{J(J+1)\hbar^2}{2I_\mathrm{M}} = B_\mathrm{r}J(J+1), \tag{2.20}$$

where $B_\mathrm{r} = \hbar^2/2I_\mathrm{M}$ is known as the **rotational constant**.

With these approximations the effective potential becomes,

$$V_\mathrm{eff} = E_\mathrm{e}(R_0) + B_\mathrm{r}J(J+1)\hbar^2 + \frac{1}{2}K\left(R-R_0\right)^2 = \mathrm{const} + \frac{1}{2}K\left(R-R_0\right)^2, \tag{2.21}$$

i.e. a harmonic potential raised by a constant energy $E_\mathrm{e}(R_0) + B_\mathrm{r}J(J+1)\hbar^2$. The solution to eqn (2.15) is therefore a set of **vibrational wave functions** identical to the usual 1D harmonic oscillator wave functions,

$$\psi_{\rm v}(x) = \left(\frac{\alpha}{\sqrt{\pi}2^v v!}\right)^{1/2} H_{\rm v}(\alpha x)\exp\left[-\frac{(\alpha x)^2}{2}\right] \tag{2.22}$$

$$\text{where} \qquad \alpha = \sqrt{\frac{\mu\omega_v}{\hbar}}, \tag{2.23}$$

and $x = R - R_0$.

The total energy[3] of the molecule is equal to the energy of a harmonic oscillator, raised by the energy $E_{\rm e}(R_0) + B_{\rm r}J(J+1)$:

$$E = E_{\rm e}(R_0) + (v+1/2)\hbar\omega_{\rm v} + B_{\rm r}J(J+1) \qquad \text{where} \quad v = 0,1,2,3,\ldots \quad J = 0,1,2,3,\ldots \tag{2.24}$$

where $\omega_{\rm v} = \sqrt{K/\mu}$ is the vibrational constant.

Note that $\omega_{\rm v}$ and $B_{\rm r}$ are in general different for different electronic states, since they depend on the electronic potential energy curve.

2.1.2 Summary

In making the Born–Oppenheimer approximation we wrote the molecular wave function as a product of an electronic and vibrational wave function. By assuming that the electronic wave function depends only weakly on the nuclear separation, the Schrödinger equation for the molecule could be separated into an electronic wave equation describing the electronic motion in the field of fixed nuclei, with eigenvalue $E_{\rm e}(R)$, and a nuclear equation describing the motion of the nuclei in the potential $E_{\rm e}(R)$. Since the potential in which the nuclei move is spherically symmetric, the nuclear wave functions could be written as a product of angular and radial parts. Hence the total energy of the molecule is the sum of three terms: an electronic energy, a vibrational energy, and a rotational energy. As we argued in lecture 1, these three contributions to the energy are significantly different in order of magnitude, such that $E_{\rm e} \gg E_{\rm v} \ggg E_{\rm r}$; indeed the validity of the Born–Oppenheimer approximation depends on this being so.

2.2 Electronic structure of diatomic molecules

We now consider the electronic wave function in more detail. We note first that for an atom, within the central-field approximation $\left[\hat{l}^2, \hat{\mathcal{H}}\right] = 0$ and $\left[\hat{l}_z, \hat{\mathcal{H}}\right] = 0$. Hence l and m_l are good quantum numbers, and the atomic orbitals can be labelled by $|nlm_lm_s\rangle$. Note that there is degeneracy in m_l, m_s.

Now imagine forming a molecule by bringing two atoms A and B together. For large R the electron orbitals will correspond to those for the separate atoms; for small R the orbitals will tend to those of the *combined atom*.[4] Now, as R is decreased from large values:

- The spherical symmetry of the atomic potential is removed.
- An additional electric field develops, which is symmetric about the internuclear axis (an axis we will call z).
- Some or all of the valence electrons become associated with *both* nuclei.
- Levels which were degenerate in the isolated atoms can split.

As a consequence of the loss of spherical symmetry, l is no longer a good quantum number in a molecule (i.e. $\left[\hat{l}^2, \hat{\mathcal{H}}\right] \neq 0$). *However*, l_z, the component of $\boldsymbol{l}$ along the internuclear axis, *does* commute with the Hamiltonian and hence m_l remains a good quantum number. The energy of molecular orbitals depends on the magnitude of m_l since this affects the spatial distribution of charge relative to the two nuclei. However, the energy is independent of the *sign* of m_l since the energy of the orbital is independent of the *direction* of rotation about the internuclear axis. As a consequence, for molecular orbitals we introduce the quantum number,

$$\lambda = |m_l| = 0,1,2,\ldots. \tag{2.25}$$

These orbitals are doubly-degenerate (apart from $\lambda = 0$).

Molecular orbitals and electronic states are labelled by the following code:

[3] In other words, the eigenvalue of eqn (2.16) with $V_{\rm eff}(R)$ given by eqn (2.21).

[4] For example, for the H_2^+ ion the molecular orbitals at small R must look like those of the He^+ ion.

	l or λ or Λ				
	0	1	2	3	...
atoms	s	p	d	f	...
mol. orbitals	σ	π	δ	ϕ	...
Electronic states	Σ	Π	Δ	Φ	...

Note molecular orbitals are labelled $(nl)\lambda$, where nl is the orbital of the *united* atom (ie. combined nuclei) OR $\lambda(nl)$, where nl is the orbital of the electron in the *separated* atoms.

2.2.1 Electronic states in multi-electron molecules

Just as for atoms, electron-electron repulsion means that the z-component of orbital angular momentum of each electron, $\hat{l}_z$, no longer commutes with the Hamiltonian. However, the z-component, $\hat{L}_z$, of the *total* orbital angular momentum $\hat{\boldsymbol{L}}$ *does*. Hence for multi-electron molecules the electronic levels are labelled by the total orbital angular momentum along the internuclear axis $\Lambda = 0, 1, 2, \ldots$

It is worth noting that the coupling of the individual orbital angular momenta to the internuclear axis is usually stronger than the coupling of the $\boldsymbol{l}_i$ to each other: in this case in the vector model the $\boldsymbol{l}_i$ precess independently about the internuclear axis, and the possible values of Λ is given by the algebraic sum of the values of l_z (which can be positive or negative). Hence a pair of π electrons can yield $\Lambda = 2$ or $\Lambda = 0$, but *not* $\Lambda = 1$.

As in atoms, we may also form the total spin $\boldsymbol{S} = \sum_i \boldsymbol{s}_i$. The electron spins do not couple to the electric field along the internuclear axis, and hence the total spin is calculated in the same way it would be for an atom. The energies of the electronic states depend on S for the same reasons it does in atoms: the spatial distribution of the electrons depends on the symmetry of the spatial part of the wave function, which in turn depends on the symmetry of the spin wave function since the total wave function must be antisymmetric with respect to electron label exchange.

Electronic levels of multi-electron molecules are labelled: ${}^{2S+1}\Lambda$, similar to the labelling of terms in an atom.

Note that we have not considered magnetic interactions, of which there are several. For example, the motion of the electrons about the internuclear axis gives rise to a magnetic field along this axis, and to which the electron spin can couple (i.e. a spin-orbit interaction). The rotation of the molecule also creates a magnetic field. As a consequence the orbital angular momentum, electron spin, and nuclear rotation can couple in numerous ways depending on the relative strengths of their interactions. These coupling schemes, known as Hund's cases, are beyond the level of the present course.

2.2.2 Symmetries of electronic states

For any diatomic molecule $\hat{\mathcal{H}}$ is unaffected by a reflection of the coordinate system in a plane which contains the internuclear axis. Let $\hat{A}_y$ be the operator for reflection in the plane $y = 0$. It can be shown that,

$$\hat{A}_y \hat{L}_z = -\hat{L}_z \hat{A}_y \tag{2.26}$$

$$\Rightarrow \left[\hat{A}_y \hat{L}_z\right] \neq 0 \qquad \text{if} \quad \hat{L}_z \neq 0. \tag{2.27}$$

Hence we cannot form simultaneous eigenfunctions of $\hat{A}_y$, $\hat{L}_z$, and $\hat{\mathcal{H}}$ for states with $\Lambda \neq 0$. We therefore choose to form simultaneous eigenfunctions of $\hat{L}_z$, and $\hat{\mathcal{H}}$, i.e. states labelled by Λ (or λ) and energy. *However*, for σ states ($\lambda = 0$), simultaneous eigenfunctions *can* be formed, to give the following non-degenerate states:

$$\sigma^+, \sigma^- \qquad \text{or} \quad \Sigma^+, \Sigma^-. \tag{2.28}$$

Homonuclear molecules

Homonuclear molecules have an additional centre of symmetry at the centre of mass, i.e. $\hat{\mathcal{H}}$ is not changed under the parity operation $\boldsymbol{r}_i \rightarrow -\boldsymbol{r}_i$. As we already saw for the case of the hydrogen molecular ion, in homonuclear molecules the levels are labelled "g" (gerade) if the electronic wave function does not change sign under the parity operator and "u" (ungerade) if the wave function does change of sign.

As an example of the labelling of electronic wave functions, and their associated potential curves, Fig. 2.2 shows the potential curves for the H_2 molecule. Note that it is common for the lowest bound electronic

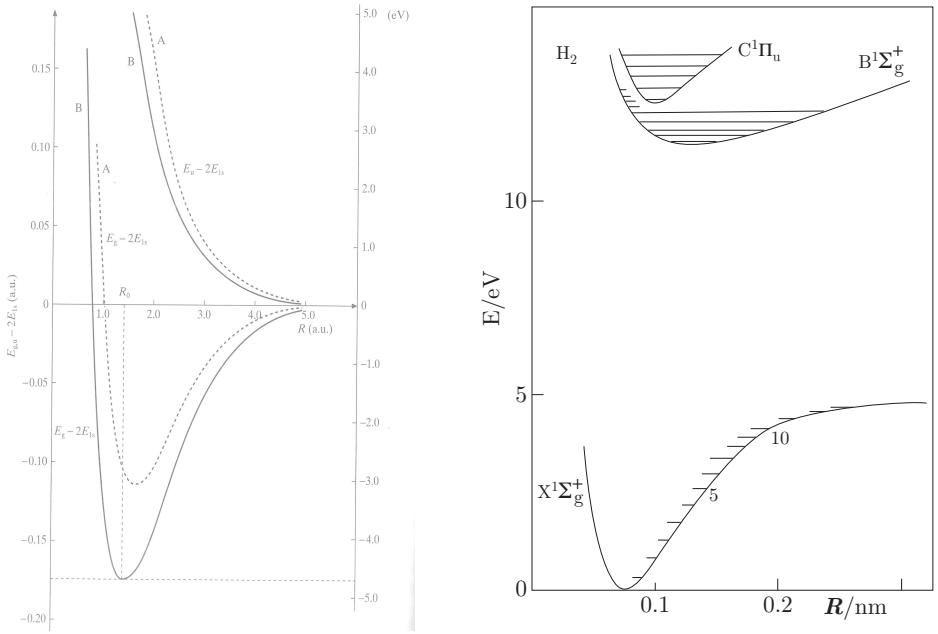

(a) (b)

Figure 2.2: Electronic potential curves of the H_2 molecule. (a) The $^1\Sigma_g^+$ and $^3\Sigma_u^+$ potential curves arising from the lowest-energy configuration, which at the limit of large R forms two ground-state hydrogen atoms. The dashed and solid potential curves arise from different approximations used to calculate them. (b) The ground and some of the excited electronic potential curves.

curve to be labelled "X", and for the excited curves to be labelled "A", "B", "C" etc., but be aware that this convention is not always followed.

Lecture 3

Radiative Transitions and Spin Statistics

3.1 Radiative transitions in molecules

The rate of electric dipole transitions is proportional to,

$$|D_{21}|^2 = \left|\left\langle \Psi' \left| -\boldsymbol{D}\cdot\hat{\boldsymbol{E}}_0 \right| \Psi'' \right\rangle\right|^2, \tag{3.1}$$

where (as is conventional in molecular physics) single and double primes indicate the upper and lower level respectively, $\hat{\boldsymbol{E}}_0$ is a unit vector pointing in the direction of the electric field of the radiation, and the dipole operator is given by (we'll leave the hat off the operator $\boldsymbol{D}$ since we will later use $\hat{\boldsymbol{D}}$ to indicate a unit vector in the direction of $\boldsymbol{D}$),

$$\boldsymbol{D} = e\left(Z_1\boldsymbol{R}_A + Z_2\boldsymbol{R}_B - \sum_j \boldsymbol{r_j}\right) = \boldsymbol{D}_{\rm n} + \boldsymbol{D}_{\rm e}. \tag{3.2}$$

We investigate this by writing out the integrals:

$$\begin{aligned} D_{21} &= \int\int \psi_{\rm e'}(\boldsymbol{R},\boldsymbol{r})\psi_{\rm n'}(\boldsymbol{R})\left[\boldsymbol{D}\cdot\hat{\boldsymbol{E}}_0\right]\psi_{\rm e''}(\boldsymbol{R},\boldsymbol{r})\psi_{\rm n''}(\boldsymbol{R})\mathrm{d}\tau_{\rm e}\mathrm{d}\tau_{\rm n} \\ &= \int \psi_{\rm n'}(\boldsymbol{R})\left\{\int \psi_{\rm e'}(\boldsymbol{R},\boldsymbol{r})\boldsymbol{D}\psi_{\rm e''}(\boldsymbol{R},\boldsymbol{r})\mathrm{d}\tau_{\rm e}\right\}\cdot\hat{\boldsymbol{E}}_0\psi_{\rm n''}(\boldsymbol{R})\mathrm{d}\tau_{\rm n}, \end{aligned}$$

It is useful first to consider the term in curly brackets:

$$\boldsymbol{D}_{\epsilon',\epsilon''}(\boldsymbol{R}) = \int \psi_{\rm e'}(\boldsymbol{R},\boldsymbol{r})\boldsymbol{D}\psi_{\rm e''}(\boldsymbol{R},\boldsymbol{r})\mathrm{d}\tau_{\rm e} \tag{3.3}$$

$$\approx \boldsymbol{D}_{\epsilon',\epsilon''}(\boldsymbol{R}_0) = \int \psi_{\rm e'}(\boldsymbol{R_0},\boldsymbol{r})\boldsymbol{D}\psi_{\rm e''}(\boldsymbol{R_0},\boldsymbol{r})\mathrm{d}\tau_{\rm e}, \tag{3.4}$$

where the approximation is valid because we expect the electronic wave function to be a slow function of R (Born–Oppenheimer approximation).

We now have,

$$D_{21} \approx \boldsymbol{D}_{\epsilon',\epsilon''}(\boldsymbol{R}_0)\int \psi'_{\rm n}(\boldsymbol{R})\left[\hat{\boldsymbol{D}}\cdot\hat{\boldsymbol{E}}_0\right]\psi''_{\rm n}(\boldsymbol{R})\mathrm{d}\tau_{\rm n}, \tag{3.5}$$

where $\hat{\boldsymbol{D}}$ is the unit vector in the direction of $\boldsymbol{D}_{\epsilon',\epsilon''}(\boldsymbol{R})$.

If we now substitute for the nuclear wave functions,

$$D_{21} \approx \boldsymbol{D}_{\epsilon',\epsilon''}(\boldsymbol{R}_0) \int \frac{1}{R}\psi_{\mathrm{v}'}(R)\frac{1}{R}\psi_{\mathrm{v}''}(R)R^2\mathrm{d}R \int \psi_{\mathrm{r}'}(\Theta,\Phi)\left[\hat{\boldsymbol{D}}\cdot\hat{\boldsymbol{E}}_0\right]\psi_{\mathrm{r}''}(\Theta,\Phi)\sin\Theta\mathrm{d}\Theta\mathrm{d}\Phi \tag{3.6}$$

$$\approx \overbrace{\boldsymbol{D}_{\epsilon',\epsilon''}(\boldsymbol{R}_0)}^{\text{electronic}} \overbrace{\int \psi_{\mathrm{v}'}(R)\psi_{\mathrm{v}''}(R)\mathrm{d}R}^{I_{\mathrm{v}},\ \text{vibl}} \overbrace{\int \psi_{\mathrm{r}'}(\Theta,\Phi)\left[\hat{\boldsymbol{D}}\cdot\hat{\boldsymbol{E}}_0\right]\psi_{\mathrm{r}''}(\Theta,\Phi)\sin\Theta\mathrm{d}\Theta\mathrm{d}\Phi}^{I_{\mathrm{r}},\ \text{rotational}}, \tag{3.7}$$

3.1.1 Transitions involving no change of electronic state

Transitions of this type *are only observed in heteronuclear molecules*, since for *homonuclear* molecules $\boldsymbol{D}_{\epsilon',\epsilon''}(\boldsymbol{R}) = 0$ because:

- $\boldsymbol{D}_{\mathrm{n}} = 0$, since $\boldsymbol{R}_A = -\boldsymbol{R}_B$
- $\boldsymbol{D}_{\mathrm{e}}$ will give zero contribution since electronic wave functions have a definite parity.

There are two types of transitions which can occur with no change of electronic state.

Pure rotational transitions

For these transitions there is no change of vibrational state (as well as no change of electronic state). Hence the integral $I_{\mathrm{v}} = 1$ because the upper and lower vibrational wave functions are identical.

The strength of the transitions are therefore determined by the integral involving the rotational transitions. The selection rules are found to be:

$$\Delta J = \pm 1. \tag{3.8}$$

Note that for pure rotational transitions absorption correspond to $\Delta J = +1$, and emission to $\Delta J = -1$. (For pure rotational transitions $\Delta J = 0$ corresponds to no transition at all!)

Ro-vibrational transitions

Transitions may also occur when both the rotational and vibrational quantum numbers change (whilst the electronic state of the two levels is the same).

If the Born-Oppenheimer approximation holds rigorously, then these transitions are forbidden since within an electronic state the vibrational wave functions are orthogonal and hence $I_{\mathrm{v}} = 0$. However, in practice $\boldsymbol{D}_{\epsilon',\epsilon''}(\boldsymbol{R})$ is not independent of $\boldsymbol{R}$ and instead,

$$\boldsymbol{D}_{\epsilon',\epsilon''}(R) = \boldsymbol{D}_{\epsilon',\epsilon''}(R_0) + \left.\frac{\mathrm{d}\boldsymbol{D}_{\epsilon',\epsilon''}}{\mathrm{d}R}\right|_{R_0}(R - R_0) + \ldots. \tag{3.9}$$

This additional dependence on $R - R_0$ introduces new terms proportional to:

$$\int \psi_{\mathrm{v}'}(R)(R - R_0)\psi_{\mathrm{v}''}(R)\mathrm{d}R \tag{3.10}$$

which is non-zero for $v'' = v' \pm 1$, corresponding to a selection rule $\Delta v = \pm 1$. Higher-order terms in the expansion of eqn (3.9) will give rise to transitions governed by selection rules $\Delta v = \pm 2$, $\Delta v = \pm 3$ etc. These higher-order transitions will generally be weaker.

For Σ electronic states the selection rule for the rotational quantum number is $\Delta J = \pm 1$. This leads to two branches: the **P-branch**, for which $\Delta J = +1$, and the **R-branch**, for which $\Delta J = -1$. Here the sign of ΔJ is defined for the transition *in emission*, i.e. $\Delta J = J'' - J'$.

For electronic states with $\Lambda \neq 0$, ro-vibrational transitions with $\Delta J = 0$ are allowed in addition to $\Delta J = \pm 1$ transitions. These form a **Q-branch** lying between the P- and R-branches; the Q-branch transitions all have the same frequency, determined by the difference in energy of the vibrational levels.

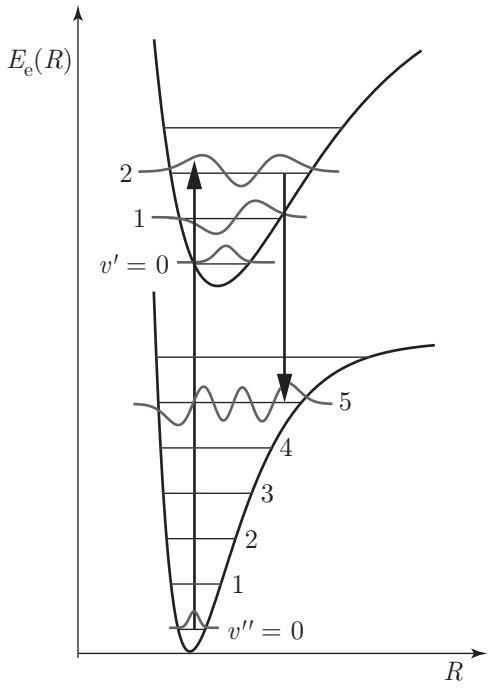

Figure 3.1: Illustration of the Franck-Condon principle.

3.1.2 Change of electronic state

If the transition involves a change in electronic state then $\boldsymbol{D}_{\epsilon',\epsilon''}(R)$ can be non zero for homonuclear molecules as well as for heteronuclear molecules since the upper and lower electronic wave functions will be different.

The selection rules may be deduced by considering eqn (3.7). Here we simply state them:

$$\Delta S = 0 \tag{3.11}$$
$$\Delta\Lambda = 0, \pm 1 \tag{3.12}$$
$$\Delta J = 0, \pm 1 \quad \text{but} \quad \Delta J \neq 0 \quad \text{if} \, \Lambda = \Lambda' = 0 \tag{3.13}$$
$$\Sigma^+ \rightarrow \Sigma^+ \quad \text{and} \quad \Sigma^- \rightarrow \Sigma^- \tag{3.14}$$
$$\mathrm{g} \rightarrow \mathrm{u}, \tag{3.15}$$

where the last two lines apply only to Σ states and homonuclear molecules respectively.

For transitions between a given pair of electronic levels, the strength of different **vibrational bands** — i.e. different pairs of vibrational quantum number for the upper and lower level — depends on the **Franck-Condon factor** $q_{v',v''}$ where,

$$q_{v',v''} = \left| \int \psi_{\mathrm{v}'}(R) \psi_{\mathrm{v}''}(R) \mathrm{d}R \right|^2, \tag{3.16}$$

which follows directly from eqn (3.7). Note that now the vibrational wave functions belong to different electronic states and hence the Franck-Condon factor is *not* necessarily zero.

The Franck-Condon principle says that the vibrational band will be strong if there is a large overlap of the vibrational wave functions in the upper and lower levels, and will be weak if that is not the case. Figure 3.1 shows schematically how the Franck-Condon factors determine the relative strength of vibrational bands. Imagine first absorption from the lower electronic level, which will occur predominantly from the lowest vibrational level ($v'' = 0$) since that will have by far the largest thermal population. The vibrational wave function for the $v'' = 0$ level will be Gaussian curve centred on the equilibrium internuclear separation, R_0, of the lower electronic level. If the two electronic levels had the same equilibrium internuclear separation, the strongest overlap of the upper and lower level vibrational wave functions would occur for the $v' = 0 \leftarrow v'' = 0$ transition since the two $v = 0$ vibrational wave functions would comprise two Gaussian functions of similar width centred at the same value of R_0. However, Since the two electronic levels have different values of

R_0, the overlap of the vibrational wave functions is maximized (in this example) for the $v' = 2 \leftarrow v'' = 0$ transition since the peak of the lower vibrational wave function approximately coincides with the large peak in the $v' = 2$ vibrational wave function of the upper electronic state.

By a similar argument, emission from the $v' = 2$ vibrational level will be dominated by transitions to both the $v'' = 0$ level and the $v'' = 5$ level since the vibrational overlaps are large for both pairs of vibrational wave functions. See Section 8.3.2 for another example of the Franck-Condon Principle.

Note that it is often said that the strongest vibrational bands occur for "vertical" transitions, i.e. transitions for which R does not change, because the vibrational motion is "frozen" during the radiative transition. However, this is not the case since the "duration" of the transition can be taken to be of the order of the radiative lifetime of the transition, which is typically 10 - 100 ns, or longer. This is *long* compared to the vibrational frequency, which is of the order of 100 fs.

3.2 Effect of nuclear spin

In atoms the coupling of the nuclear spin to the magnetic field generated by the spins and orbital motion of the electrons causes hyperfine structure. The same phenomenon also occurs in molecules, leading to a small splitting of energy levels. We will ignore this hyperfine structure and concentrate instead on a much more profound effect which arises in *homonuclear* diatomic molecules because of the requirement that the total wave function of the molecule must have a definite symmetry with respect to exchange of the nuclei. In particular, if the nuclei are bosons the wave function must be symmetric with respect to exchange; if the nuclei are fermions it must be antisymmetric.

Let the total molecular wave function be written as

$$\Psi_{\rm tot} = \Psi(\boldsymbol{R}, \boldsymbol{r})\chi_{\rm N}(1,2), \tag{3.17}$$

where $\Psi(\boldsymbol{R}, \boldsymbol{r})$ is the wave function of the molecule we have considered so far, including the electron spin, and $\chi_{\rm N}(1,2)$ is the nuclear spin wave function.

Exchange of the nuclei corresponds to the operation $\boldsymbol{R} \rightarrow -\boldsymbol{R}$. As shown in Fig. 3.2 the operation $\boldsymbol{R} \rightarrow -\boldsymbol{R}$ corresponds to:

- Rotation by 180° of the molecule about an axis normal to the internuclear axis. Let us call this rotation axis y.
- Reflection in a plane containing the internuclear axis (i.e. $y \rightarrow -y$).
- Inversion of electron co-ordinates ($\boldsymbol{r}_i \rightarrow -\boldsymbol{r}_i$).

By considering these processes in turn it is easy to see that the *electronic wave functions* have the following symmetry with respect to exchange of the nuclei:[1]

$$\text{Symmetric:} \qquad \Lambda_{\rm u}^-, \Lambda_{\rm g}^+ \tag{3.18}$$

$$\text{Antisymmetric:} \qquad \Lambda_{\rm g}^-, \Lambda_{\rm u}^+ \tag{3.19}$$

The vibrational wave function depends only on $|\boldsymbol{R} - \boldsymbol{R_0}|$ and so is unaltered by $\boldsymbol{R} \rightarrow -\boldsymbol{R}$. Similarly the electronic spin wave function is unchanged by the operation $\boldsymbol{R} \rightarrow -\boldsymbol{R}$.

The rotational wave functions have the following symmetries:

$$\text{Symmetric:} \qquad J \text{ is even} \tag{3.20}$$

$$\text{Antisymmetric:} \qquad J \text{ is odd} \tag{3.21}$$

We can therefore summarize the symmetry properties of the wave function $\Psi(\boldsymbol{R}, \boldsymbol{r})$ as follows:

	g^+	g^-	u^+	u^-
J even	S	A	A	S
J odd	A	S	S	A

[1] Previously we argued that for $\Lambda > 0$ simultaneous eigenfunctions of the Hamiltonian, $\hat{L}_z$ and $\hat{A}_y$ could not be formed. It is beyond the present syllabus, but for completeness we note that interactions between the rotational and electronic motions can lift the two-fold degeneracy of $\Lambda > 0$ levels to form states with definite reflection symmetry. In such cases the electronic states are labelled as in eqns (3.18) and (3.19) even if $\Lambda > 0$. For example, magnetic interactions can form non-degenerate $\Pi_{\rm g}^+$, $\Pi_{\rm g}^-$, $\Pi_{\rm u}^+$ and $\Pi_{\rm u}^-$ states.

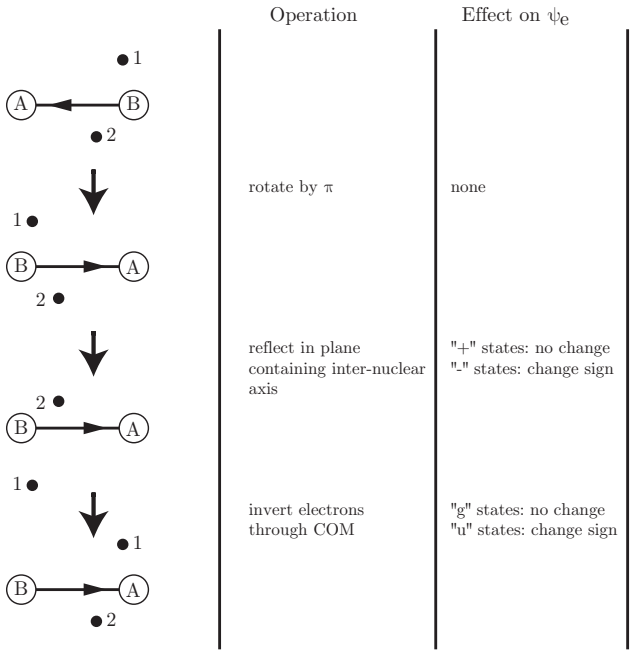

Figure 3.2: Effect of exchange of nuclei on electronic wave functions.

These symmetry requirements lead to some profound effects, as discussed below.

3.2.1 Examples

Nuclei with $I = 0$

In this case the total molecular wave function must be symmetric with respect to exchange of the nuclei. In addition, since $I = 0$, only one nuclear spin wave function exists — this is symmetric with respect to exchange of nuclei. As a consequence, only half of the rotational levels can exist!

For example, ^{16}O has a ground state of $^3\Sigma_g^-$, which is antisymmetric on exchange of nuclei. Hence *only rotational levels with odd J can exist*; even-J levels are missing. It is therefore found that alternate transitions in the rotational fine structure are missing. However, if one of the nuclei is replaced by ^{17}O, there is no longer a requirement for the wave function to have a definite symmetry with respect to exchange of nuclei, and the missing lines are restored.

Molecular hydrogen

As a second example we consider $^1H_2$, which has $I = 1/2$ and hence can have a total nuclear spin $T = 0$ or $T = 1$. Transitions between $T = 0$ and $T = 1$ states are extremely rare, and hence hydrogen behaves as if there are two types of H_2 molecule: "ortho-hydrogen" ($T = 1$) and "para-hydrogen" ($T = 0$).

The ground electronic state of H_2 is Σ_g^+ and hence only the following combinations have the required anti-symmetry with respect to exchange of the nuclei:

$$T = 0: \quad \text{'para'} \qquad \chi_N^A = \frac{1}{\sqrt{2}} [\uparrow\downarrow - \downarrow\uparrow] \qquad \text{even J} \tag{3.22}$$

$$T = 1: \quad \text{'ortho'} \qquad \chi_N^S = \begin{cases} \uparrow\uparrow \\ \frac{1}{\sqrt{2}} [\uparrow\downarrow + \downarrow\uparrow] \\ \downarrow\uparrow \end{cases} \qquad \text{odd J} \tag{3.23}$$

The statistical weight of ortho-hydrogen ($T = 1$) is 3 times that of para ($T = 0$), leading to a 3:1 ratio of intensities in the rotational fine structure.

In general, for a diatomic molecule with identical nuclei of spin I, the intensities of the rotational fine structure have a ratio of $(I + 1)/I$. This forms the basis of an important method of determining nuclear spins.

Lecture 4

Conditions for optical gain

4.1 Review of Einstein description

As you will have seen, the interaction of radiation and matter may be described by a semi-classical treatment. Providing the linewidth of the transition is sufficiently large, and the intensity of the radiation is not too high, the semi-classical treatment gives identical results to the Einstein treatment. In practice the Einstein approach is found to be valid for the conditions found inside virtually all lasers, leading to the use of so-called **rate equations** to describe the population densities in the energy levels of the laser.

Einstein considered two levels of an atom, an upper level of energy E_2, and a lower level of energy E_1. He identified three processes by which radiation could interact with atoms in these levels. The first is **spontaneous emission**, in which an atom in the upper level decays to the lower level by the emission of a photon with energy $\hbar\omega_{21} = E_2 - E_1$. The spontaneously emitted photon can be emitted in any direction.

The second and third processes are **absorption**, in which an atom in the lower level is excited to the upper level by the absorption of a photon of energy $\hbar\omega_{21}$; and **stimulated emission**, in which an incident photon of energy $\hbar\omega_{21}$ stimulates an atom in the upper level to decay to the lower level by the emission of a second photon of energy $\hbar\omega_{21}$. The stimulated photon is emitted into the same mode as the incident photon, and hence has the same frequency, direction, and polarization as the incident photon. This third process, stimulated emission, is the key to the operation of the laser.

It seems reasonable that the rate of spontaneous emission should be independent of the conditions of the radiation field in which the atom finds itself. Furthermore, it is clear that the rates at which absorption and stimulated emission occur must depend in some way on the density of photons of energy $\hbar\omega_{21}$, or, equivalently, on the energy density of the radiation field at ω_{21} . In three postulates Einstein went further and stated that the rates of absorption and stimulated emission are *linearly* dependent on the energy density at ω_{21}. The Einstein postulates may be stated as follows:

1. The rate per unit volume at which atoms in the upper level 2 decay spontaneously to the lower level 1 is equal to $N_2 A_{21}$, where N_2 is the number of atoms per unit volume in level 2, and A_{21} is a constant characteristic of the transition;

2. The rate per unit volume at which atoms in the lower level are excited to the upper level by the absorption of photons of energy $\hbar\omega_{21}$ is equal to $N_1 B_{12}\rho(\omega_{21})$, where N_1 is the number of atoms per unit volume in level 1, $\rho(\omega_{21})$ is the energy density of radiation of angular frequency ω_{21} and B_{12} is a constant characteristic of the transition;

3. The rate per unit volume at which atoms in the upper level decay to the lower level by the stimulated emission of photons of energy $\hbar\omega_{21}$ is equal to $N_2 B_{21}\rho(\omega_{21})$, where B_{21} is a constant characteristic of the transition.

The coefficients A_{21}, B_{12}, and B_{21} are known as **the Einstein A and B coefficients**. The three fundamental interactions between atoms and radiation are shown schematically in Fig. 4.1.

Note: The energy density $\rho(\omega_{21})$ appearing in the definition of the Einstein coefficients is a spectral quantity, but the population densities are total population densities (having units of atoms per unit volume). Hence the units of A_{21} are simply s^{-1}, whilst those of B_{12} and B_{21} are $\mathrm{m}^3\,\mathrm{J}^{-1}\,\mathrm{rad}\,\mathrm{s}^{-2}$.

There is an important subtlety here. We have assumed that the levels of the atom have perfectly defined energies, and as such only interact with radiation at exactly ω_{21}. In practice, however, the atomic levels will always be broadened to some extent. We will see later how to adapt the Einstein approach to deal with broadened levels.

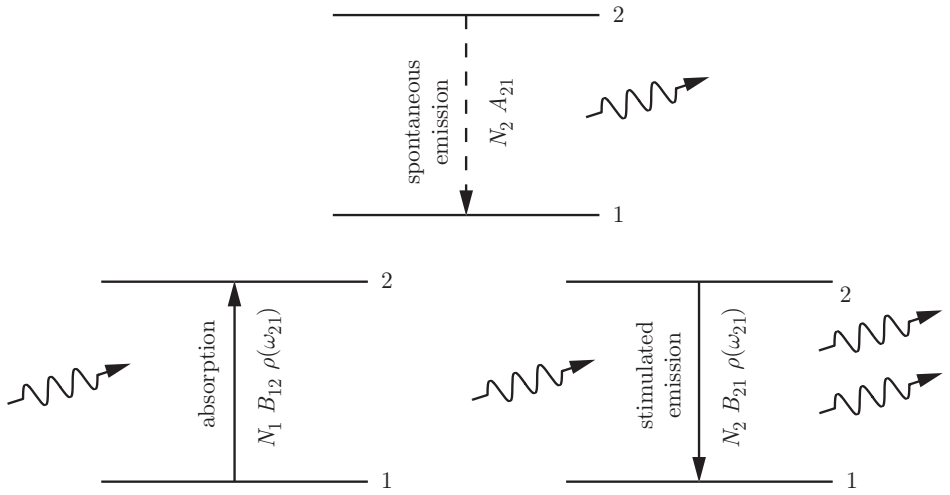

Figure 4.1: Illustration of the interaction of radiation with two levels of an atom by spontaneous emission, absorption, and stimulated emission. For each process the transition rates are given in terms of the Einstein coefficients and the number densities N_2 and N_1 of atoms in the upper and lower levels. The photons have energy $\hbar\omega_{21}$ and the figure should be read from left to right. For example, in the case of stimulated emission an incident photon of energy $\hbar\omega_{21}$ stimulates an excited atom to make a transition to the lower level, emitting a second photon in the process.

4.1.1 Relations between the Einstein coefficients

As you saw in an earlier lecture, relations between the Einstein coefficients may be found by considering the case of an atom in thermal equilibrium with a radiation field of temperature T. This approach leads to the following relations:

$$g_1 B_{12} = g_2 B_{21} \tag{4.1}$$

$$A_{21} = \frac{\hbar\omega_{21}^3}{\pi^2 c^3} B_{21}, \tag{4.2}$$

where g_i is the degeneracy of level i. It is important to realize that, by construction, the Einstein coefficients are properties of the atomic levels, and not the radiation field. As such, these relations hold for *any* radiation field (not just blackbody) and whether or not the atoms are in thermal equilibrium.

4.2 Conditions for gain

As we will see more formally later, for **l**ight **a**mplification by the **s**timulated **e**mission of **r**adiation we require the rate of stimulated emission to be greater than the rate of absorption:

$$N_2 B_{21} \rho(\omega_{21}) > N_1 B_{12} \rho(\omega_{21})$$

$$\Rightarrow \frac{N_2}{g_2} > \frac{N_1}{g_1} \qquad \textbf{Condition for optical gain} \tag{4.3}$$

In other words, the population **per state** must be greater in the upper level than in the lower level, a situation called a **population inversion**.

We should realize that a population inversion is unusual. If the level populations, for example, were in thermal equilibrium at temperature T the populations of the levels would be described by a Boltzmann distribution:

$$\frac{N_2}{N_1} = \frac{g_2}{g_1} \exp\left(-\frac{E_2 - E_1}{k_B T}\right), \tag{4.4}$$

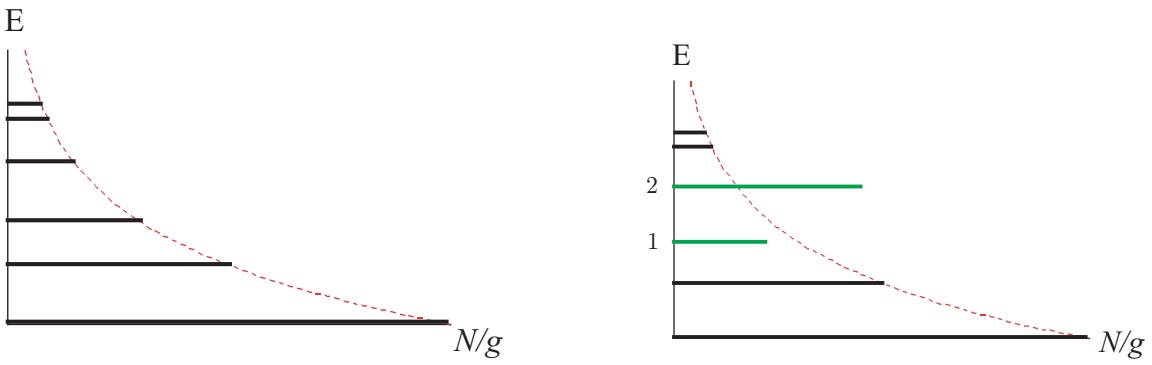

Figure 4.2: Comparison of the populations per state for (a) an atom in thermal equilibrium; (b) an atom with a population inversion between levels 2 and 1.

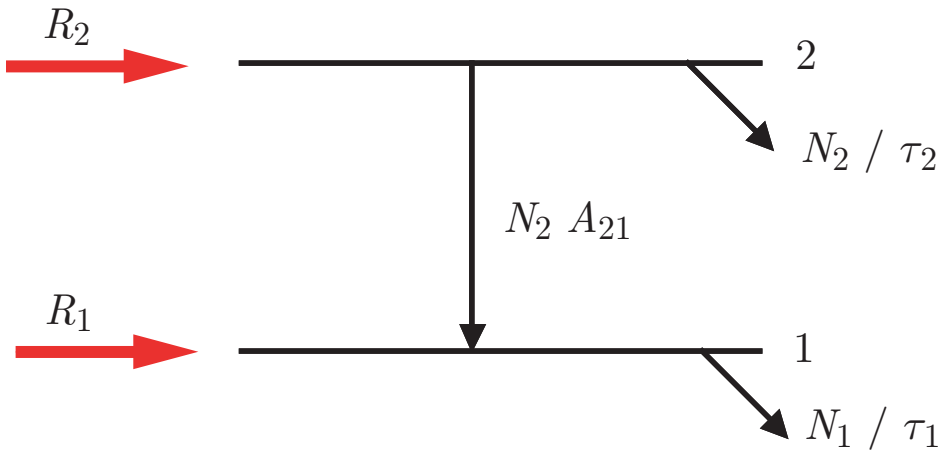

Figure 4.3: Rate equation analysis of the condition for establishing steady-state gain on the transition 2 → 1.

or,

$$\frac{N_2/g_2}{N_1/g_1} = \exp\left(-\frac{E_2 - E_1}{k_B T}\right). \tag{4.5}$$

from which it is clear that for a system in thermal equilibrium the population per state of an upper level is always lower than that for any lower-lying level. Figure 4.2 illustrates schematically the distribution over levels for (a) thermal equilibrium and (b) a population inversion between levels 2 and 1.

4.2.1 Conditions for steady-state inversion

Having demonstrated that a population inversion cannot exist under conditions of thermal equilibrium, it is useful to explore the conditions under which a population inversion can be produced. Figure 4.3 shows schematically the kinetic processes which affect the populations of the upper and lower levels of a laser transition. We suppose that atoms in the upper level are produced, or 'pumped' at a rate R_2 (units of atoms $\mathrm{m}^{-3}\,\mathrm{s}^{-1}$), and that the lifetime of the upper level is τ_2. Note that the pump rate includes all processes that excite the upper level such as direct optical pumping, electron collisional excitation, and radiative and non-radiative cascade from higher-lying levels. The lifetime τ_2 is the lifetime against all types of decay (radiative, collisional de-excitation, etc.) and includes radiative decay to level 1. It is known as the **fluorescence lifetime**, since it is the lifetime with which the strength of the fluorescence on any radiative transition from level 2 would be observed to decay. We define the pump rate and lifetime of the lower laser level in a similar way, but do not include spontaneous emission on the laser transition itself in R_1. That contribution to the population of level 1 will be handled explicitly, for reasons that will be clear below.

The evolution of the population densities in the two levels may then be written as,

$$\frac{\mathrm{d}N_2}{\mathrm{d}t} = R_2 - \frac{N_2}{\tau_2} \tag{4.6}$$

$$\frac{\mathrm{d}N_1}{\mathrm{d}t} = R_1 + N_2 A_{21} - \frac{N_1}{\tau_1}. \tag{4.7}$$

Note that the symmetry of the two equations is broken by the spontaneous emission term, $N_2 A_{21}$. It is straightforward to solve the above for steady-state conditions by setting $dN_2/dt = dN_1/dt = 0$. We find,

$$N_2 = R_2 \tau_2 \tag{4.8}$$

$$N_1 = R_1 \tau_1 + R_2 \tau_2 A_{21} \tau_1. \tag{4.9}$$

For optical gain we require $N_2/g_2 > N_1/g_1$ which yields the following condition for a steady-state population inversion:

$$\frac{R_2}{R_1}\frac{\tau_2}{\tau_1}\frac{g_1}{g_2}\left[1 - \frac{g_2}{g_1}A_{21}\tau_1\right] > 1. \qquad \textbf{Steady-state inversion} \tag{4.10}$$

As discussed in Section 4.2.2, the term in square brackets must be less than or equal to unity. By considering the case when it takes its largest value (i.e. 1), we conclude that for a steady-state population inversion to be achieved at least one of the following must be true:

Selective pumping $R_2 > R_1$: in which the upper laser level is pumped more rapidly than the lower laser level;

Favourable lifetime ratio $\tau_2 > \tau_1$: in which the lower laser level decays more rapidly than the upper level, which keeps the population of the lower level small;

Favourable degeneracy ratio $g_1 > g_2$: which ensures that the population per state of the lower laser level is small.

4.2.2 Necessary, but not sufficient condition

As mentioned above, the factor in square brackets in eqn (4.10) must be less than one; in fact it can be negative as well as positive, and is independent of the pumping rates, depending only on the parameters of the laser transition. In other words, for some systems no matter how selective the pumping is it is not possible to achieve a steady-state population inversion. The reason for this somewhat surprising result is that increasing the population of the upper laser level by pumping harder also increases the rate at which the lower level is populated by spontaneous emission on the laser transition itself.

This final factor in eqn (4.10) therefore yields **a necessary, but not sufficient condition** for achieving a steady-state population inversion. The condition that this factor is positive can be re-written as,

$$A_{21} < \frac{g_1}{g_2}\frac{1}{\tau_1}. \qquad \textbf{necessary, but not sufficient condition} \tag{4.11}$$

Hence the rate of spontaneous decay from the upper to the lower laser level must be smaller than the total rate of decay from the lower laser level (multiplied by a factor of g_1/g_2). In other words, the lower level has to empty sufficiently quickly for population not to build up by spontaneous emission on the laser transition.

It should be stressed that satisfying eqn (4.11) does not ensure that a steady-state population inversion will be achieved on a given transition. For example the pumping may not preferentially populate the upper laser level, or the lifetime ratio may be very unfavourable. However, unless eqn (4.11) is satisfied, no pumping technique, no matter how selective, will be able to create a steady-state population inversion on the transition.[1]

[1] Of course, it might be that a population inversion is created for a short period — a "transient" inversion — but it will not be possible to generate a steady-state inversion unless eqn (4.11) is satisfied.

Lecture 5

Line broadening

5.1 Introduction

So far we have assumed that the upper and lower levels of a transition are infinitely sharp, and consequently the radiation emitted in transitions between them is monochromatic. In reality, of course, that is not the case and for any given transition a number of mechanisms can lead to broadening of the radiation emitted.

5.2 Homogeneous line broadening

5.2.1 Natural broadening

According the quantum model of atoms and molecules considered so far, the energy levels of these systems are stationary states. Consequently an atom in such a state would remain in the state forever, unless it was subject to a perturbation of some kind. However, we know from experiment that atoms and molecules in excited states *can* decay spontaneously in the absence of an external field. The resolution of this discrepancy requires that we also treat the radiation field quantum mechanically; this is beyond the present course, and hence we will introduce radiative decay phenomenologically.

We saw earlier in the course that an electromagnetic wave, with a frequency reasonably close to the transition frequency ω_{21} causes the wave function of a two-level atom to become,

$$\psi(\boldsymbol{r},t) = c_1(t)\phi_1(\boldsymbol{r})\exp(-\mathrm{i}E_1t/\hbar) + c_2(t)\phi_2(\boldsymbol{r})\exp(-\mathrm{i}E_2t/\hbar), \tag{5.1}$$

where E_1 and E_2 are the energies of the upper and lower levels and c_1 and c_2 describe how the probability of finding the atom in a given state varies with time.

It is interesting to consider the following matrix element:

$$\begin{aligned}
\boldsymbol{p}(t) &= \langle\psi(\boldsymbol{r},t)| - e\boldsymbol{r}\,|\psi(\boldsymbol{r},t)\rangle & (5.2)\\
&= \exp\left(\mathrm{i}\frac{E_2-E_1}{\hbar}t\right)\langle c_1\phi_1| - e\boldsymbol{r}\,|c_2\phi_2\rangle + \text{c.c.} & (5.3)\\
&+ |c_1|^2\langle\phi_1| - e\boldsymbol{r}\,|\phi_1\rangle + |c_2|^2\langle\phi_2| - e\boldsymbol{r}\,|\phi_2\rangle & (5.4)\\
&= \exp\left(\mathrm{i}\frac{E_2-E_1}{\hbar}t\right)\langle c_1\phi_1| - e\boldsymbol{r}\,|c_2\phi_2\rangle + \text{c.c.}, & (5.5)
\end{aligned}$$

where c.c. means complex conjugate of the preceding term, and the last line follows from the fact that $\langle\phi_1| - e\boldsymbol{r}\,|\phi_1\rangle = \langle\phi_2| - e\boldsymbol{r}\,|\phi_2\rangle = 0$. The quantity $\boldsymbol{p}(t)$ corresponds to a dipole moment oscillating at the transition frequency $\omega_{21} = (E_2 - E_1)/\hbar$. Hence we can consider an atom[1] undergoing a radiative transition as forming an electric dipole oscillating at the transition frequency ω_{21}.

We now assume that the effect of spontaneous decay of the upper and lower levels leads to exponential damping of $\boldsymbol{p}(t)$ i.e.

$$\boldsymbol{p}(t) = \boldsymbol{p}(0)\exp\left(-\frac{\gamma}{2}t\right)\cos(\omega_0 t). \tag{5.6}$$

[1] From hereon we will use the term 'atoms' to refer to both atoms and molecules, unless otherwise specified.

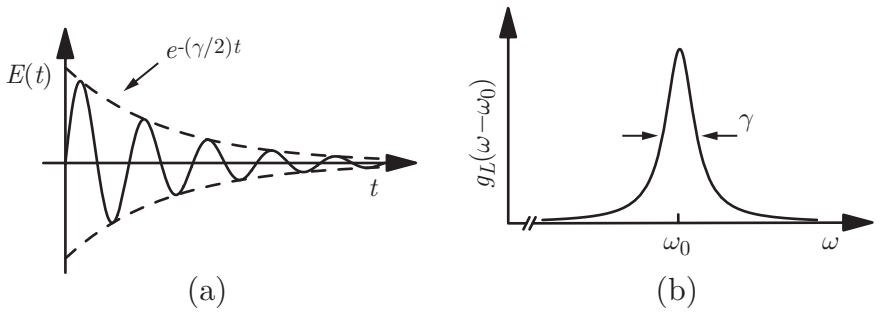

Figure 5.1: Illustrating how a damped oscillating electric field from a damped oscillating dipole (a) gives rise to a frequency spectrum with a Lorentzian profile (b).

We would therefore expect that in the far-field the electric field radiated by the atom will be proportional to $\mathrm{d}\boldsymbol{p}/\mathrm{d}t$, and hence will be of the form:

$$\mathbf{E}(t) = \mathbf{E}(0)\exp\left(-\frac{\gamma}{2}t\right)\sin(\omega_0 t). \tag{5.7}$$

The frequency distribution of the oscillating electric field is given by the Fourier Transform of $E(t)$, which we will denote by E_ω. We see immediately that the spectrum will consist of a range of frequencies owing to the fact that the electric field is not a pure harmonic wave. Now, the signal from any detection system able to measure the emitted spectrum will be proportional to $|E_\omega|^2$. By calculating the Fourier Transform we find,

$$|E_\omega|^2 \propto g_{\mathrm{L}}(\omega-\omega_0) = \frac{1}{\pi}\frac{\gamma/2}{(\omega-\omega_0)^2+(\gamma/2)^2}. \tag{5.8}$$

The function $g_{\mathrm{L}}(\omega-\omega_0)$ is known as the **lineshape function** and is normalized[2] such that $\int_0^\infty g_{\mathrm{L}}(\omega-\omega_0)\mathrm{d}\omega = 1$. The full-width at half-maximum (FWHM)) of the lineshape is found straightforwardly from eqn (5.8) to be,

$$\Delta\omega_{\mathrm{N}} = \gamma. \tag{5.9}$$

The width $\Delta\omega_{\mathrm{N}}$ is known as the **natural (or lifetime) broadened linewidth**, for the reasons outlined below.

Relation to the lifetimes of the levels

For eqn (5.9) to be useful we need to relate the damping constant γ to measured properties of the transition. To do this we first consider an ensemble of atoms all initially excited to an upper level k. As illustrated in Fig. 5.2, the atoms can decay spontaneously to a range of lower levels $\ldots l, m, n \ldots$. The rate equation for the population of atoms in level k is simply,

$$\begin{aligned}\frac{\mathrm{d}N_k}{\mathrm{d}t} &= -N_k A_{kl} - N_k A_{km} - N_k A_{kn} - \ldots \\ &= -N_k \sum_{E_i<E_k} A_{ki}.\end{aligned} \tag{5.10}$$

Hence the population of atoms in the excited level decays exponentially according to,

$$N_k(t) = N_k(0)\exp\left(-\frac{t}{\tau_k^{\mathrm{rad}}}\right), \tag{5.11}$$

where the **radiative lifetime** is given by,

[2]Actually the function $g_{\mathrm{L}}(x)$ is normalized such that $\int_{-\infty}^{\infty} g_{\mathrm{L}}(x)dx = 1$. In eqn (5.8) the argument of $g_{\mathrm{L}}(x)$ extends only to $-\omega_0$. However, since the linewidth is always very small compared to ω_0, extending the lower limit to $-\infty$ will have negligible effect on the integral.

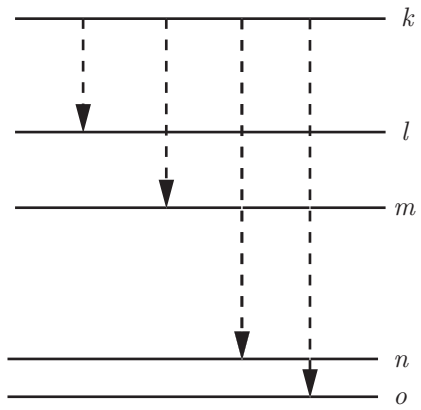

Figure 5.2: Radiative decay of an excited level k to lower levels $\ldots l, m, n \ldots$

$$\frac{1}{\tau_k^{\rm rad}} = \sum_{E_i<E_k} A_{ki}. \tag{5.12}$$

Clearly the energy stored in atoms in the upper level will decay according to $\exp(-t/\tau_k^{\rm rad})$. Remembering that a classical dipole has an energy proportional to $p(t)^2$, and hence has an energy which decays as $\exp(-\gamma t)$, and taking into account the effect of the decay of the *lower* level, we conclude that the natural linewidth of the transition $k \to j$ is given by

$$\Delta\omega_{\rm N} = \gamma = \frac{1}{\tau_k^{\rm rad}} + \frac{1}{\tau_j^{\rm rad}} \qquad \text{Natural linewidth} \tag{5.13}$$

We note that the upper level of any radiative transition must have a finite lifetime. Hence, irrespective of the lifetime of the lower level, radiative transitions must have a minimum spectral width determined by eqn (5.13). Since it is an intrinsic property of the transition, the broadening arising from the finite lifetime of the upper and lower levels is often known as **natural broadening**,

5.2.2 Pressure broadening

Radiation emitted by a sample of atoms in the gaseous phase will be homogeneously broadened as a result of collisions with other atoms, electrons, ions etc. This is known as **pressure broadening**.

We may extend the simple model above to the case of pressure broadening in an intuitively obvious way. We suppose that a radiating atom emits a damped wave of the form of eqn (5.7) until such time it experiences a collision at a time τ_i whereupon the atom stops radiating. As before, the frequency distribution of the radiated wave is given by the Fourier transform of the radiated electric field. Now, however, the spectrum will be modified and, in particular, will depend on how long the atom radiates before it makes a collision. From our knowledge of Fourier Transforms we can guess that if τ_i is short the spectrum will be wide in frequency, whereas if the atom radiates for a long time before suffering a collision the frequency width will essentially be the natural width.

Now, the spectrum observed from a macroscopic sample of atoms will be given by averaging the spectra over the distribution of times between collisions. From Kinetic Theory we know that these times are distributed according to

$$P(\tau_i)\mathrm{d}\tau_i = \exp\left(-\frac{\tau_i}{\tau_{\rm c}}\right)\frac{\mathrm{d}\tau_i}{\tau_{\rm c}}, \tag{5.14}$$

where $\tau_{\rm c}$ is the mean time between collisions.

Working through this analysis we find that the lineshape is once more Lorentzian, but now the width is modified to,

$$\Delta\omega_{\rm p} = \gamma + \frac{2}{\tau_{\rm c}}. \qquad \textbf{Pressure-broadened linewidth} \tag{5.15}$$

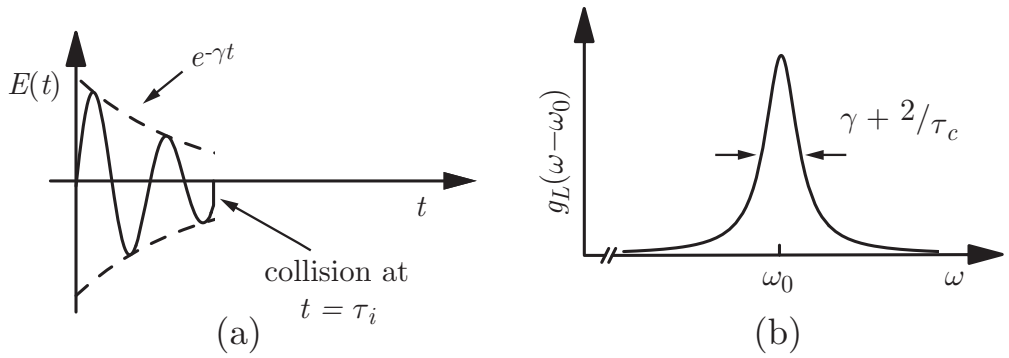

Figure 5.3: A simple model of collision broadening. A damped oscillating dipole is subject to a collision, leading to the electric field shown in (a). When averaged over the distribution of collision times, this gives rise to a frequency spectrum with a Lorentzian profile (b).

Note the factor of 2 in the second term.

Clearly the linewidth in this case increases as the mean time between collisions decreases. Typically τ_c is inversely proportional to the pressure of the gas, in which case the increase in linewidth is proportional to pressure. For obvious reasons, this type of broadening is known as **pressure broadening**. The process is illustrated schematically in Fig. 5.3

It is important to note that collisions which do not de-excite the atom, but only perturb the *phase* of the atomic wave functions, also cause spectral broadening. In many circumstances these phase-changing collisions occur more frequently than those causing the atom to change energy level, and hence are more important in determining the width of the spectral line.

5.2.3 Phonon broadening

In many solid-state lasers the active species are ions doped into a crystalline host. The energy level structure of ions in a crystalline environment is generally different (sometimes very different) than that of an isolated ion owing to interactions with the surrounding ions of the lattice. These interactions can be described in terms of a crystal electric field which, for a perfect crystal at zero temperature, will have a symmetry reflecting that of the crystal lattice.

The crystal field splits and shifts the energy levels from their positions in the isolated ion to give a rich energy level structure. Since the positions of the energy levels depends on the locations of the neighbouring ions, thermal motion of the crystal lattice causes the energy levels of the dopant ion to fluctuate about their zero-temperature positions. The time-scale of thermal oscillations of the lattice is very fast (of order picoseconds, as for diatomic molecules), and hence the energy levels appear to be smeared out, or broadened. Broadening of a large number of close-lying levels split by the crystal field can give rise to broad, essentially continuous energy bands.

The thermal vibrations of the lattice are quantized, the quantum of acoustic energy being termed a **phonon**. As such this thermal broadening can also be described as a collision process, analogous to pressure broadening, in which phonon collisions cause broadening by: (i) removing population from the levels by absorption or emission of phonons; (ii) perturbing the phase of the wave functions of the levels. Phase-changing collisions are usually more rapid than population-changing collisions, and hence typically dominate phonon broadening. Thermal broadening in crystals is therefore often known as **phonon broadening**.

A third type of phonon broadening occurs in **vibronic transitions** in which the transition from an upper to a lower level occurs through the simultaneous emission of a photon and one or more phonons. Since the energy taken up by the phonon(s) can vary, the energy of the photon must change to conserve energy; this leads to extensive broadening, which is utilized in several wavelength tunable lasers such as Ti:sapphire.

It is also worth noting that collisions of phonons with ions in excited states can cause the ion to decay to lower-lying levels without the emission of radiation. In **non-radiative decays** of this type the energy difference is carried away by lattice phonons. As we will see, non-radiative decay plays a crucial role in forming and maintaining the population inversion in many solid-state laser systems.

Finally we note that, as we might expect, both the degree of phonon broadening and the non-radiative decay rates of excited ions depend strongly on the temperature and material of the lattice.

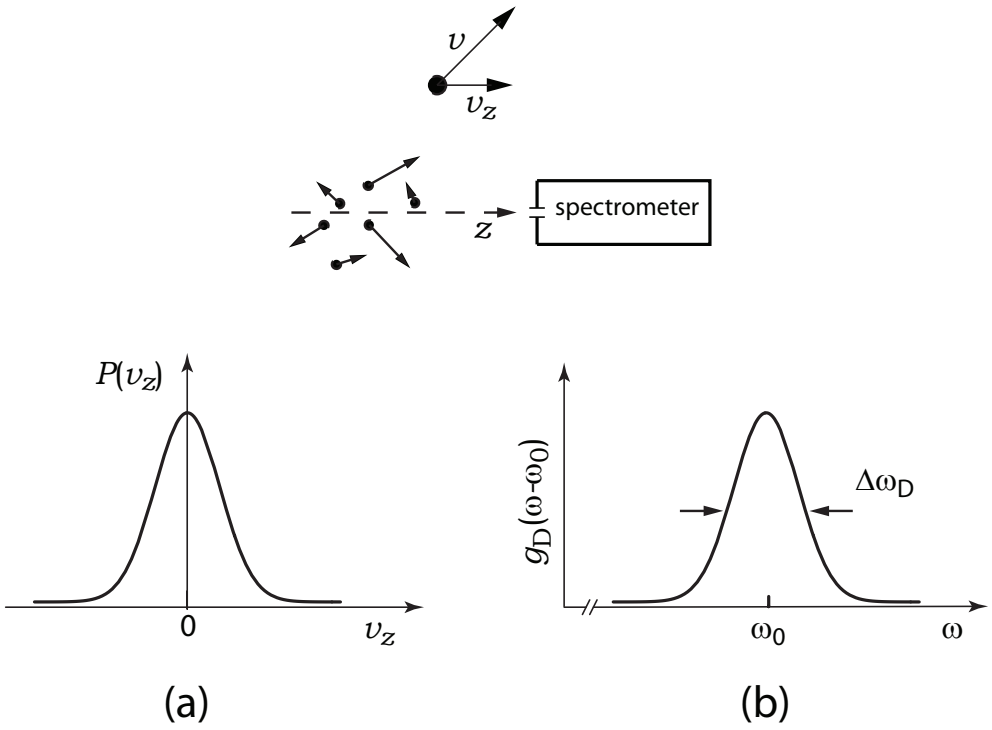

Figure 5.4: The formation of an inhomogeneously broadened spectral line by Doppler-broadened gas atoms. Radiation emitted by the atoms in the z-direction is detected by the spectrometer. The distribution of atomic velocities in the z-direction (a) leads, via the Doppler effect, to a distribution of frequencies measured by the spectrometer, and hence broadening of the spectral line (b).

5.3 Inhomogeneous broadening

The homogeneous broadening mechanisms discussed above affect all atoms in a sample equally, so that the distribution of frequencies emitted by any atom in the sample is the same. However, other broadening mechanisms exist which cause the transition frequency of different atoms to be shifted by different amounts. Such broadening mechanisms are said to be **inhomogeneous**, the broadening being characterized by a distribution of transition frequencies $g_{\rm D}(\omega-\omega_0)$.[3]

Inhomogeneous broadening will always be associated with some homogeneous broadening since natural broadening is always present, and the atoms may also be subject to other homogeneous broadening mechanisms such as phonon broadening. However, it should be clear that when, as is often the case, the frequency width of the inhomogeneous distribution $g_{\rm D}(\omega-\omega_0)$ is much greater than that of the homogeneous distribution $g_{\rm H}(\omega-\omega_0)$ the observed transition lineshape will simply be the inhomogeneous lineshape.

5.3.1 Doppler broadening

For gas lasers the most important line broadening mechanism is very often **Doppler broadening**, which arises from a combination of the Doppler effect and the thermal motion of the atoms.

Imagine using a spectrometer to measure the emission spectrum on a certain transition from a gaseous sample of atoms, as illustrated schematically in Fig. 5.4. We ignore homogeneous broadening and assume that stationary atoms emit a single frequency ω_0. Consider now the radiation emitted by those atoms travelling with a velocity v_z towards the spectrometer. The observed frequency ω, i.e. that measured by the spectrometer, will be shifted from the frequency ω_0 emitted by a stationary atom according to,

$$\omega-\omega_0=\frac{v_z}{c}\omega_0, \tag{5.16}$$

where we have ignored relativistic effects since for all cases of interest to lasers $v_z \ll c$.

We see that those atoms moving towards the spectrometer will appear to emit higher frequencies, whilst the frequencies measured for those atoms moving away from the spectrometer will be lower than ω_0. As-

[3] We have used the superscript 'D' rather than 'I' to distinguish the inhomogeneous lineshape from the homogeneous lineshape in order to avoid possible confusion with the use of the subscript 'I' used to indicate saturation effects. The inhomogeneous lineshape defined here applies to any form of inhomogeneous broadening, not just Doppler broadening.

suming that the sample is in thermal equilibrium with temperature T, the proportion $P(v_z)\mathrm{d}v_z$ of atoms with a z-component of velocity in the range v_z to $v_z + \mathrm{d}v_z$ is given by the **Maxwellian distribution**:

$$P(v_z)\mathrm{d}v_z = \sqrt{\frac{M}{2\pi k_\mathrm{B} T}} \exp\left(-\frac{M v_z^2}{2 k_B T}\right) \mathrm{d}v_z, \tag{5.17}$$

where M is the mass of each atom, and k_B the Boltzmann constant.

Substitution of eqn (5.16) into eqn (5.17) gives the observed lineshape $g_\mathrm{D}(\omega - \omega_0)$:

$$g_\mathrm{D}(\omega - \omega_0)\mathrm{d}\omega = \sqrt{\frac{M}{2\pi k_\mathrm{B} T}} \exp\left(\frac{-Mc^2}{2 k_\mathrm{B} T}\left[\frac{\omega - \omega_0}{\omega_0}\right]^2\right) \frac{c}{\omega_0}\mathrm{d}\omega. \tag{5.18}$$

This is a Gaussian distribution with a full-width at half maximum, known as the Doppler width, given by:

$$\Delta\omega_\mathrm{D} = 2\sqrt{2\ln 2}\frac{\omega_0}{c}\sqrt{\frac{k_\mathrm{B} T}{M}}, \tag{5.19}$$

$$\frac{\Delta\omega_\mathrm{D}}{\omega_0} = \frac{\Delta\nu_\mathrm{D}}{\nu_0} = 7.16 \times 10^{-7}\sqrt{\frac{T}{A}}, \tag{5.20}$$

Doppler width

where in eqn (5.20) the temperature is in Kelvin and the atomic mass A has units of grammes per mole.

It is usually more convenient to re-write the lineshape[4] in terms of $\Delta\omega_\mathrm{D}$, i.e.

$$g_\mathrm{D}(\omega - \omega_0) = \frac{2}{\Delta\omega_\mathrm{D}}\sqrt{\frac{\ln 2}{\pi}} \exp\left(-\left[\frac{\omega - \omega_0}{\Delta\omega_\mathrm{D}/2}\right]^2 \ln 2\right), \tag{5.21}$$

Normalized Gaussian lineshape

where the distribution is normalized so that $\int_0^\infty g_\mathrm{D}(\omega - \omega_0)d\omega = 1$.

5.3.2 Broadening in amorphous solids

As discussed above, transitions within ions doped into a solid will be broadened by phonon interactions. If the host is a good quality single crystal, this broadening is homogeneous. However if the solid is highly non-uniform, active ions in different locations will experience different environments. Of particular importance is the local value of the strain of the crystal lattice since this affects the local crystal field experienced by the ion, which in turn affects the energy levels of the ion through the Stark effect. Other aspects of the local environment which can affect the transition frequencies of an active ion are the presence of impurity ions, or variations in the orientation of the crystal lattice. Since such affects change the centre frequency of the active ions according to their location in the medium, the broadening of the frequency response of a macroscopic sample is inhomogeneous.

These effects are particularly important for ions doped in glasses, such as Nd^{3+} ions in the Nd:glass laser, since in a glassy material the local environment varies very widely with position, leading to substantial inhomogeneous broadening. Very often the distribution of centre frequencies is found to follow a Normal, i.e. Gaussian, distribution, in which case the transition lineshape is also Gaussian.

5.4 Homogeneous vs inhomogeneous broadening

Line broadening mechanisms can be divided into two classes: **homogeneous broadening** and **inhomogeneous broadening**. A homogeneous broadening mechanism is one which affects all atoms in the sample equally, and consequently all atoms will interact with a beam of radiation of frequency ω with the same strength.

In contrast, an inhomogeneous broadening mechanism causes the frequency of a transition to be different for different 'types' of atom; the distribution of different 'types' leads to an observed broadening when the emission or absorption of the whole sample is viewed. For example, in Doppler broadening the transition frequency of an atom depends on its velocity with respect to the observer (or a beam of radiation). The

[4] Whilst we have considered the lineshape of the radiation emitted from the sample, we could also have considered the absorption spectrum that would be measured and we would have found the same distribution $g_\mathrm{D}(\omega - \omega_0)$.

spectrum emitted by a sample of moving atoms will be broadened according to the distribution of relative velocities.

The key test in deciding if a broadening mechanism is homogeneous or inhomogeneous is whether a narrow-band beam of radiation will interact with all atoms equally (homogenous) or not (inhomogeneous).

Lecture 6

The optical gain cross-section

6.1 Homogeneous broadening and the Einstein coefficients

Our original discussion of the Einstein treatment assumed that the energy levels were perfectly sharp. We now discuss how to adapt this approach to the more realistic case in which the transition is broadened. We will only consider the case of homogeneous broadening.

For a system of homogeneously broadened atoms, all atoms will interact with a beam of radiation of angular frequency ω with the same strength. However, the strength of the interaction will depend on the detuning of ω from ω_0, the centre frequency of the transition.

We can account for this by incorporating the frequency dependence into spectral lineshapes:

1. The rate per unit volume at which atoms in the upper level decay to the lower level by spontaneous emission of photons with angular frequencies lying in the range ω to $\omega + \delta\omega$ is equal to

$$N_2 A_{21} g_A(\omega - \omega_0)\delta\omega,$$

   where N_2 is the density of atoms in the upper level and $g_A(\omega - \omega_0)$ is the lineshape for spontaneous emission.

2. The rate per unit volume at which atoms in the lower level are excited to the upper level by the absorption of photons with angular frequencies lying in the range ω to $\omega + \delta\omega$ is equal to

$$N_1 B_{12} g_B(\omega - \omega_0)\rho(\omega)\delta\omega,$$

   where N_1 is the density of atoms in the lower level, $g_B(\omega - \omega_0)$ is the lineshape for absorption, and $\rho(\omega)$ is the spectral energy density of the radiation.

3. The rate per unit volume at which atoms in the upper level decay to the lower level by stimulated emission of photons with angular frequencies lying in the range ω to $\omega + \delta\omega$ is equal to

$$N_2 B_{21} g_{B'}(\omega - \omega_0)\rho(\omega)\delta\omega,$$

   where $g_{B'}(\omega - \omega_0)$ is the lineshape for stimulated emission.

For the moment, we have allowed the frequency dependence of the three processes to be different. Notice also that the lineshapes must be normalized, which ensures that when integrated over the entire lineshape of the transition the total rates of spontaneous emission, absorption, and stimulated emission agree with the Einstein coefficients. For example, the total rate of spontaneous emission at all frequencies is given by,

$$\int_0^\infty N_2 A_{21} g_A(\omega - \omega_0)\mathrm{d}\omega = N_2 A_{21}. \tag{6.1}$$

Similar relations hold for the lineshapes for absorption and stimulated emission.

The question remains, how are the different lineshapes related? By considering the rate of emission and absorption of photons with angular frequencies lying in the range ω to $\omega + \delta\omega$ for a system of matter in thermal equilibrium with radiation, as in our earlier derivation of the relations between the Einstein coefficient, we may derive relations between the rates of the three fundamental processes:

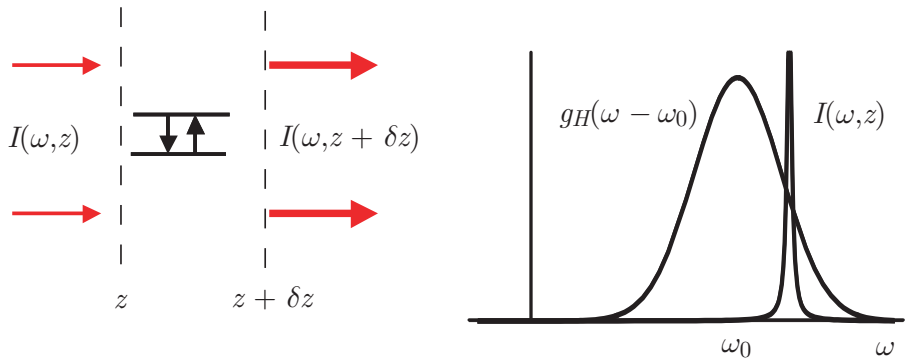

Figure 6.1: Derivation of the optical gain cross-section for a homogeneously-broadened transition.

$$g_1 B_{12} g_B(\omega - \omega_0) = g_2 B_{21} g_{B'}(\omega - \omega_0) \tag{6.2}$$

$$A_{21} g_A(\omega - \omega_0) = \frac{\hbar\omega_0^3}{\pi^2 c^3} B_{21} g_{B'}(\omega - \omega_0). \tag{6.3}$$

We see immediately that the lineshapes for absorption and spontaneous and stimulated emission are identical; in other words the three processes all have the same frequency dependence.

But what *is* that frequency dependence? In Lecture 2 we derived the lineshapes $g_{\rm H}(\omega - \omega_0)$ for spontaneous emission in the presence of various types of homogeneous broadening. However, by the definitions above, spontaneous emission has a lineshape given by $g_A(\omega - \omega_0)$. Hence we see that the lineshapes $g_A(\omega - \omega_0) = g_B(\omega - \omega_0) = g_{B'}(\omega - \omega_0)$ are just equal to the emission lineshape $g_{\rm H}(\omega - \omega_0)$. For example, for lifetime-broadened transitions $g_{\rm H}(\omega - \omega_0)$ would be the Lorentzian function of eqn (5.8).

6.2 Optical gain

We are now in a position to describe how a beam of radiation may be amplified.

Suppose that the beam propagates along the $z-$axis through a medium with population densities N_2 and N_1 in the upper and lower levels respectively. In general the radiation will have a finite spectral width, and is described by a spectral intensity $I(\omega, z)$ and energy density $\rho(\omega, z)$. We take the laser transition to be homogeneously broadened so that all atoms interact with the beam equally.

We consider the amplification of the beam as it passes through the small region lying between the planes $z = z$ and $z = z + \delta z$, as illustrated schematically in Fig. 6.1. As the beam passes through the medium it loses energy owing to absorption by atoms in the lower laser level, but gains energy by stimulated emission from atoms in the upper laser level. The net rate at which atoms are transferred from the upper to the lower laser level by the stimulated emission of photons with angular frequencies lying between ω and $\omega + \delta\omega$ is,

$$[N_2 B_{21} - N_1 B_{12}] g_{\rm H}(\omega - \omega_0) \rho(\omega, z) \delta\omega \cdot A \delta z \tag{6.4}$$

where A is the area of the beam. Each such transfer releases an energy of $\hbar\omega$ to the beam, and hence, within this frequency range, the power gained by the beam is,

$$[N_2 B_{21} - N_1 B_{12}] g_{\rm H}(\omega - \omega_0) \rho(\omega, z) \delta\omega \cdot A \delta z \cdot \hbar\omega. \tag{6.5}$$

For the frequency interval under consideration, the power carried into the region by the beam is $I(\omega, z) A \delta\omega$, and hence the power gained by the beam can also be written as,

$$[I(\omega, z + \delta z) - I(\omega, z)] A \delta\omega. \tag{6.6}$$

Equating eqns. (6.5) and (6.6) we find, straightforwardly,

$$\frac{\partial I}{\partial z} = [N_2 B_{21} - N_1 B_{12}] g_{\rm H}(\omega - \omega_0) \frac{\hbar\omega}{c} I(\omega, z), \tag{6.7}$$

where we have used the fact that for a beam of radiation $I(\omega, z) = \rho(\omega, z)$c. This result is usually tidied in the following form:

$$\frac{\partial I}{\partial z} = N^* \sigma_{21}(\omega - \omega_0) I(\omega, z), \tag{6.8}$$

where we have used the relation between the Einstein B-coefficients and defined the **population inversion density** as,

$$N^* = N_2 - \frac{g_2}{g_1} N_1, \tag{6.9}$$

and the **optical gain cross-section** as[1],

$$\sigma_{21}(\omega - \omega_0) = \frac{\hbar \omega_0}{c} B_{21} g_{\mathrm{H}}(\omega - \omega_0) \tag{6.10}$$

$$\Rightarrow \sigma_{21}(\omega - \omega_0) = \frac{\pi^2 c^2}{\omega_0^2} A_{21} g_{\mathrm{H}}(\omega - \omega_0) \tag{6.11}$$

The advantage of writing our result in the form of eqn (6.8) is that the right-hand side is now factored into terms which depend on (i) the population densities of the upper and lower levels; (ii) the atomic physics of the transition; (iii) the spectral intensity of the beam.

6.2.1 Small-signal gain coefficient

Equation (6.8) is very often re-written as,

$$\frac{1}{I} \frac{\partial I}{\partial z} = \alpha_{21}(\omega - \omega_0) \tag{6.12}$$

where $\alpha_{21}(\omega - \omega_0)$ is known as **the small-signal gain coefficient** (units m^{-1}), and is given by,

$$\alpha_{21}(\omega - \omega_0) = N^* \sigma_{21}(\omega - \omega_0). \tag{6.13}$$

We will see later that it is important to recognize that the small-signal gain coefficient is in general also a function of the beam intensity. The reason for this is that at very high intensities the increased rate of stimulated emission will reduce the population inversion, a process known as gain saturation.

For the moment we will neglect that complication and assume that the population inversion is positive and independent of intensity or position. Then, integrating eqn (6.12) we find,

$$I(\omega, z) = I(\omega, 0) \exp[\alpha(\omega - \omega_0) z], \tag{6.14}$$

We see that the beam of radiation grows exponentially with propagation distance. The reason for the energy gain of the beam is straightforward: the rate of stimulated emission from the upper level is greater than the rate of absorption from the lower level.

The small-signal gain coefficient (often loosely called 'the gain coefficient') is important in determining the performance of a laser system. Since the gain coefficient is proportional to the population inversion density, it is strongly dependent upon the operating conditions of the laser. For example, in a neodymium-doped yttrium aluminium garnet (Nd:YAG) laser the gain coefficient will depend on many parameters of the laser design including the strength of the optical pumping and the concentration of Nd^{3+} ions in the YAG crystal. In contrast the optical gain cross-section is a more fundamental parameter of the laser transition since it depends only on the physics of the laser transition and therefore is largely independent of the pumping conditions.

[1] Once again we will set $\omega \approx \omega_0$ in the factors multiplying the lineshape

6.2.2 Absorption and Beer's Law

It is worth recognizing that we can define the cross-section in various ways. The gain cross-section defined in eqn (6.10) takes the form it does because of the way we defined the population inversion. We defined $N^* = N_2 - (g_2/g_1)N_1$ since, as laser physicists, we hope that N^* will be positive. Clearly in the ideal case the population in the lower level will be small, and then $N^* \approx N_2$.

If we studied absorption, however, we would generally be interested in the lower level population. To illustrate this, suppose that the population inversion where negative and independent of intensity or position. Equation (6.14) would then take the form,

$$I(\omega, z) = I(\omega, 0) \exp\left[-\kappa_{12}(\omega - \omega_0)z\right], \tag{6.15}$$

where the **absorption coefficient** is given by,

$$\begin{aligned}
\kappa_{12}(\omega - \omega_0) &= -\left(N_2 - \frac{g_2}{g_1}N_1\right)\sigma_{21}(\omega - \omega_0) \\
&= -\left(\frac{g_1}{g_2}N_2 - N_1\right)\frac{g_2}{g_1}\sigma_{21}(\omega - \omega_0) \\
&= +\left(N_1 - \frac{g_1}{g_2}N_2\right)\frac{g_2}{g_1}\frac{\hbar\omega_0}{c}B_{21}g_{\rm H}(\omega - \omega_0) \\
&= +\left(N_1 - \frac{g_1}{g_2}N_2\right)\frac{\hbar\omega_0}{c}B_{12}g_{\rm H}(\omega - \omega_0) \\
&= +N^{**}\sigma_{12}^{\rm abs}(\omega - \omega_0)
\end{aligned} \tag{6.16}$$

where $N^{**} = N_1 - (g_1/g_2)N_2$ and the **absorption cross-section** is given by

$$\sigma_{21}^{\rm abs}(\omega - \omega_0) = (\hbar\omega_0/c)B_{12}g_{\rm H}(\omega - \omega_0). \tag{6.17}$$

Notice that the absorption cross-section follows the definition of the gain cross-section but with B_{21} replaced with B_{12}, as we might expect.

The exponential decrease in the intensity of the beam as it propagates through the medium is known as **Beer's Law**.

6.2.3 Frequency dependence of gain

In the case that N^* is independent of intensity or position, eqn (6.14) describes the growth of each frequency component. Clearly the growth in intensity depends on the detuning of the frequency from the centre frequency ω_0. The frequency dependence of the optical gain cross-section is simply the lineshape of the transition, $g_{\rm H}(\omega - \omega_0)$. So, for example, a transition which is lifetime-broadened will have an optical gain cross-section with a Lorentzian lineshape:

$$\sigma_{21}^{\rm L}(\omega - \omega_0) = \frac{\hbar\omega_0}{\rm c}B_{21}\frac{1}{\pi}\frac{(\Delta\omega_{\rm L}/2)}{(\omega - \omega_0)^2 + (\Delta\omega_{\rm L}/2)^2}, \tag{6.18}$$

where $\Delta\omega_{\rm L}$ is the FWHM of the lineshape.

Clearly the optical gain cross-section will typically be strongly peaked at the transition frequency ω_0. In the absence of saturation the beam grows as $\exp[N^*\sigma_{21}(\omega - \omega_0)z]$ and consequently the amplification of the beam will be an even stronger function of function of frequency. Hence, if a beam is input to an optical amplifier with a frequency width which is of order, or larger, than the linewidth of the transition, the spectral width of the output beam will be much narrower owing to greater amplification of frequencies close to the line centre. Frequency narrowing of this type is known as **gain narrowing**.

6.3 Laser rate equations for narrow-band radiation

The bandwidth $\Delta\omega_{\rm B}$ of the oscillating mode in a laser oscillator (i.e. a gain medium located within an optical cavity) will nearly always be very small compared to the spectral width of the laser transition. Likewise, for an amplifier (just a gain medium, with no optical cavity) it is also often the case that the bandwidth of

the beam to be amplified is narrow compared to that of the optical transition concerned. We will therefore make this simplifying assumption in what follows.

In general the rate equation for (say) the upper laser level can then be written in the form,

$$\frac{\mathrm{d}N_2}{\mathrm{d}t} = R_2 - (N_2 B_{21} - N_1 B_{12}) \int_0^\infty g_{\mathrm{H}}(\omega - \omega_0)\rho(\omega)\mathrm{d}\omega + \ldots, \tag{6.19}$$

where we see that the total rate of stimulated emission is given by integrating over the lineshape, and $+\ldots$ indicate that in general other terms may appear in the rate equation. We may re-arrange eqn (6.19) as follows:

$$\begin{aligned} \frac{\mathrm{d}N_2}{\mathrm{d}t} &= R_2 - \left(N_2 - \frac{g_2}{g_1}N_1\right) \int_0^\infty \frac{\hbar\omega}{\mathrm{c}} B_{21} g_{\mathrm{H}}(\omega - \omega_0) \frac{\rho(\omega)\mathrm{c}}{\hbar\omega}\mathrm{d}\omega + \ldots & (6.20) \\ &= R_2 - N^* \int_0^\infty \sigma_{21}(\omega - \omega_0) \frac{I(\omega)}{\hbar\omega}\mathrm{d}\omega + \ldots & (6.21) \end{aligned}$$

where $I(\omega)$ is the spectral intensity of the radiation.

For narrow-band radiation the gain cross-section varies slowly over the spectral width of the radiation and so $I(\omega)$ acts like a Dirac delta function: $I(\omega) = I_{\mathrm{T}}\delta(\omega - \omega_{\mathrm{L}})$ where I_{T} is the <u>total</u> intensity and ω_{L} the centre frequency of the beam. We then have:

$$\begin{aligned} \frac{dN_2}{dt} &= R_2 - N^* \int_0^\infty \sigma_{21}(\omega - \omega_0) \frac{I_{\mathrm{T}}\delta(\omega - \omega_{\mathrm{L}})}{\hbar\omega} d\omega + \ldots & (6.22) \\ &= R_2 - N^* \sigma_{21}(\omega_{\mathrm{L}} - \omega_0) \frac{I_{\mathrm{T}}}{\hbar\omega_{\mathrm{L}}} + \ldots, & (6.23) \end{aligned}$$

Eqn. (6.23) may be interpreted as follows. We can regard N^* as the effective number density of inverted atoms, and $\sigma_{21}(\omega_{\mathrm{L}} - \omega_0)$ as their effective cross-sectional area. Since $I_{\mathrm{T}}/\hbar\omega_{\mathrm{L}}$ is the photon flux, eqn (6.23) takes the standard form for the rate of a process in terms of a cross-section and a flux of incident particles.

6.3.1 Growth equation for a narrow-band beam

We have already derived the equation describing the growth of each spectral component of a beam (eqns (6.12) and (6.13)):

$$\frac{\partial I}{\partial z} = N^* \sigma_{21}(\omega - \omega_0) I(\omega, z). \tag{6.24}$$

To describe the rate of growth of a beam of finite spectral width we integrate both sides of the above over the bandwidth of the beam:

$$\begin{aligned} \int_0^\infty \frac{\partial I}{\partial z} d\omega &= \int_0^\infty N^* \sigma_{21}(\omega - \omega_0) I(\omega, z) d\omega \\ \Rightarrow \frac{\partial}{\partial z} \int_0^\infty I(\omega, z) d\omega &= \int_0^\infty N^* \sigma_{21}(\omega - \omega_0) I(\omega, z) d\omega \\ \Rightarrow \frac{dI_{\mathrm{T}}}{dz} &= \int_0^\infty N^* \sigma_{21}(\omega - \omega_0) I(\omega, z) d\omega. \end{aligned} \tag{6.25}$$

Again, for narrow-band radiation we may bring the cross-section outside the integral:

$$\frac{dI_{\mathrm{T}}}{dz} = N^* \sigma_{21}(\omega_{\mathrm{L}} - \omega_0) I_{\mathrm{T}}. \tag{6.26}$$

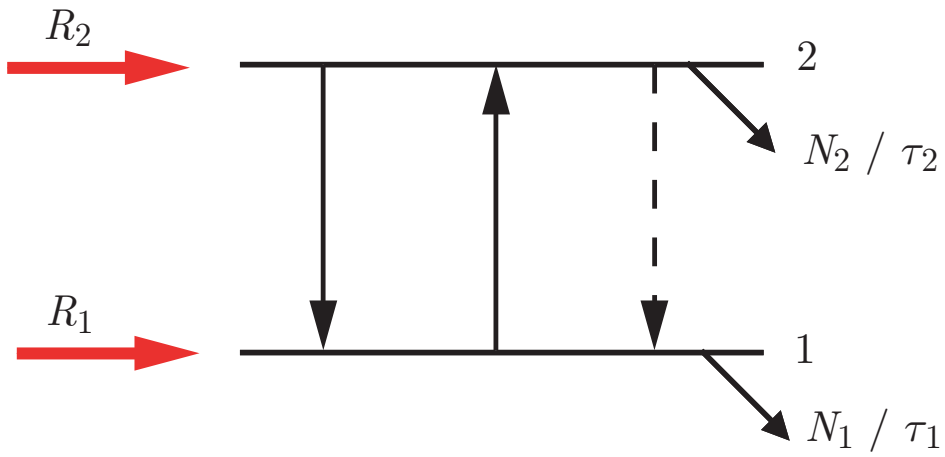

Figure 6.2: Processes affecting the upper and lower laser levels in a laser operating under steady-state conditions in the presence of an intense radiation beam.

6.4 Gain saturation

We are now consider how a beam of intense, narrow-band radiation (such as might be present in an operating laser) affects the population inversion produced by the pumping. Figure 6.2 shows schematically the processes which affect the level populations of a laser operating under steady-state conditions in the presence of an intense radiation beam.

We may write the rate equations for the laser levels as,

$$\frac{\mathrm{d}N_2}{\mathrm{d}t} = R_2 - N^*\sigma_{21}(\omega_\mathrm{L}-\omega_0)\frac{I}{\hbar\omega_\mathrm{L}} - \frac{N_2}{\tau_2} \tag{6.27}$$

$$\frac{\mathrm{d}N_1}{\mathrm{d}t} = R_1 + N^*\sigma_{21}(\omega_\mathrm{L}-\omega_0)\frac{I}{\hbar\omega_\mathrm{L}} + N_2A_{21} - \frac{N_1}{\tau_1}. \tag{6.28}$$

where we have dropped the subscript T from the total intensity[2].

We note that:

1. We will assume that the pump rates R_2 and R_1 are constant and, in particular, are independent of N_1 and N_2;
2. The pump rates include direct excitation collision rates, indirect processes such as pumping by radiative or non-radiative cascades. However, spontaneous emission on the laser transition itself is included explicitly as N_2A_{21}.

It is straightforward to find the steady-state solutions of eqns (6.27) and (6.28):

$$N_2 = R_2\tau_2 - N^*\sigma_{21}\frac{I}{\hbar\omega_\mathrm{L}}\tau_2 \tag{6.29}$$

$$N_1 = R_1\tau_1 + N^*\sigma_{21}\frac{I}{\hbar\omega_\mathrm{L}}\tau_1 + N_2A_{21}\tau_1, \tag{6.30}$$

where we have dropped the frequency dependence of $\sigma_{21}(\omega_\mathrm{L}-\omega_0)$ to avoid clutter. Eliminating N_2 from eqn (6.30) gives the population inversion density $N^* = N_2 - (g_2/g_1)N_1$ as,

$$N^* = \frac{R_2\tau_2\left[1-(g_2/g_1)A_{21}\tau_1\right] - (g_2/g_1)R_1\tau_1}{1+\sigma_{21}\frac{I}{\hbar\omega_\mathrm{L}}\left[\tau_2+(g_2/g_1)\tau_1-(g_2/g_1)A_{21}\tau_1\tau_2\right]}. \tag{6.31}$$

This last result looks complicated, but it is actually rather simple! Notice that the denominator equals unity when $I = 0$. Consequently, the numerator must be just the population inversion produced by the pumping in the absence of the beam. Hence we can rewrite eqn (6.31) in the following form:

[2]From here onwards we will always distinguish spectral intensity by writing it in the form $I(\omega)$.

$$N^*(I) = \frac{N^*(0)}{1 + I/I_\mathrm{s}}. \tag{6.32}$$

The parameter I_s is known as the **saturation intensity**, and is given by

$$I_\mathrm{s} = \frac{\hbar\omega_\mathrm{L}}{\sigma_{21}} \left(\tau_2 + \frac{g_2}{g_1}\tau_1 - \frac{g_2}{g_1} A_{21}\tau_1\tau_2 \right)^{-1}, \tag{6.33}$$

which is itself usually re-written in the form,

$$I_\mathrm{s} = \frac{\hbar\omega_\mathrm{L}}{\sigma_{21}\tau_\mathrm{R}}, \qquad \textbf{Saturation intensity} \tag{6.34}$$

in which τ_R, **the recovery time**, is given by

$$\tau_\mathrm{R} = \tau_2 + \frac{g_2}{g_1}\tau_1[1 - A_{21}\tau_2] \tag{6.35}$$

Let us consider eqn (6.32) in more detail. We see that the intense beam of radiation reduces, or 'burns down', the population inversion by a factor of $(1 + I_\mathrm{T}/I_\mathrm{s})$ as a result of the increased rate of stimulated emission from the upper laser level. The intensity of the radiation required to reduce the inversion to one-half of that achieved in the absence of the beam is the saturation intensity (units of W m^{-2}). For a laser oscillator or amplifier the saturation intensity is, then, a measure of the intensity to which a beam may be amplified before the increased rate of stimulated emission from the upper laser level starts to affect the level populations significantly. As such the saturation intensity marks the boundary between 'high' and 'low' intensity.

6.4.1 Approximations for the saturation intensity

It is often possible to find different approximations for the saturation intensity. For example, in so-called 'four-level' lasers the fluorescence lifetime of the lower level is much shorter than that of the upper level. In this special case $\tau_\mathrm{R} \approx \tau_2$. The same approximation for the recovery time occurs when the upper laser level decays predominantly by radiative decay on the laser transition itself, whereupon $\tau_2 \approx A_{21}^{-1}$. For these special cases we find,

$$I_\mathrm{s} \approx \frac{\hbar\omega_\mathrm{L}}{\sigma_{21}\tau_2} \qquad \text{Special case if} \quad \tau_2 \gg \tau_1 \quad \text{or} \quad A_{21}\tau_2 \approx 1. \tag{6.36}$$

6.4.2 Saturated gain coefficient

Having found the burnt down population inversion density, the saturated gain coefficient is found from,

$$\alpha_I(\omega - \omega_0) = N^*(I)\sigma_{21}(\omega - \omega_0), \tag{6.37}$$

where the subscript I indicates that α is now a function of the beam intensity.

Hence,

$$\alpha_I(\omega - \omega_0) = \frac{\alpha_0(\omega - \omega_0)}{1 + I/I_\mathrm{s}}, \qquad \textbf{Saturation of gain coefficient} \tag{6.38}$$

where $\alpha_0(\omega - \omega_0)$ is the small-signal gain coefficient, i.e. the gain coefficient experienced by, or measured with, a beam of intensity much less than the saturation intensity.

6.4.3 Saturated of absorption coefficient

Absorption of radiation will exhibit saturation for the same reason that gain saturates: at high intensities the radiation transfers a significant number of atoms between the levels. In the case of absorption, the radiation transfers population from the lower level (nearly always the ground state) to the upper level of the transition; at high intensities the population of the lower level is depleted, reducing the absorption.

The dependence of the absorption coefficient of a homogeneously broadened transition on the radiation intensity is analogous to that of the gain coefficient:

$$\kappa_I(\omega-\omega_0) = \frac{\kappa_0(\omega-\omega_0)}{1+I/I_\mathrm{s}}, \qquad \textbf{Saturation of absorption coefficient} \tag{6.39}$$

where $\kappa_0(\omega-\omega_0)$ is the small-signal absorption coefficient, i.e. the absorption coefficient experienced by, or measured with, a weak beam. The saturation intensity has the same form as eqn (6.34), *but* the recovery time τ_R is NOT given by eqn (6.35). The reason for this is that for the case of absorption the lower level does not decay; the recovery time therefore depends on the upper level lifetime, and also on the rate at which atoms in the upper level return to the lower level via intermediate levels.[3]

6.5 Beam growth in a laser amplifier

From the analysis above we know that a narrow-band beam of radiation will grow as it propagates through a length of inverted medium according to:

$$\frac{\mathrm{d}I}{\mathrm{d}z} = \alpha_I I = \frac{\alpha_0}{1+I/I_\mathrm{s}} I, \tag{6.40}$$

which may be integrated to give,

$$\ln\left[\frac{I(z)}{I(0)}\right] + \frac{I(z)-I(0)}{I_\mathrm{s}} = \alpha_0 z. \tag{6.41}$$

This transcendental equation has algebraic solutions in two limits:

$$I(z) = I(0)\exp(\alpha_0 z); \qquad \textbf{Weak beam } (I(z) \ll I_\mathrm{s}) \tag{6.42}$$

$$I(z) = I(0) + \alpha_0 I_\mathrm{s} z. \qquad \textbf{Heavy saturation } (I(0) \gg I_\mathrm{s}) \tag{6.43}$$

In other words, at low intensities the intensity of the beam grows exponentially with distance, just as we found earlier; whereas once the laser transition becomes heavily saturated the intensity grows linearly.

[3] See Exercise 5.3 in Hooker & Webb for details.

Lecture 7

Cavity effects

7.1 Cavity modes

A simple laser amplifier consists of one or more sections of inverted media such that a beam injected at one end is amplified as it propagates. In a laser oscillator the gain medium is located within an optical cavity, such that the laser radiation originates within the gain medium itself and is amplified as it circulates around the optical cavity. Unless qualified, the term 'laser' usually refers to a laser oscillator. In this section we examine the effect of the optical cavity on the operation and output of a laser oscillator.

Let us first consider a simple laser cavity comprising two mirrors separated by a distance L_c, as illustrated in Fig. 7.1. For the moment we will consider the case in which there is *no gain medium* within the cavity.

Suppose that radiation is circulating within the cavity. Under steady-state conditions we can represent the radiation by a wave propagating towards positive z, denoted by a subscript $+$, and a wave propagating to negative z denoted by a subscript $-$.

The positive- and negative-going waves will be one (or a superposition) of the transverse modes of the cavity. The transverse modes of the cavity are eigenmodes of the cavity which, when launched once round the cavity return with the same transverse spatial variation. As such they depend on the curvature of the cavity mirrors and their location. For the present purpose we need not concern ourselves with the detailed form of the transverse modes and we merely denote the modes of the positive- and negative-going waves by the functions $u_\pm(\boldsymbol{r}, \omega, t)$. However, in anticipation of the introduction of gain into the cavity, we will allow the overall amplitude of the positive- and negative-going waves to vary with position along the cavity axis according to $a_\pm(z, \omega)$.

Let us now consider the amplitude of the radiation field immediately to the right of mirror 1, i.e. at $z = 0$. Under steady-state conditions, after reflection from mirror 1 the negative-going wave must be the same as the right-going wave at $z = 0$. Hence we have:

$$a_+(0,\omega)u_+(\boldsymbol{r},\omega,t) = a_-(0,\omega)r_1 e^{i\phi_1} u_-(\boldsymbol{r},\omega,t). \tag{7.1}$$

where r_1 and ϕ_1 are the modulus and phase respectively of the amplitude reflection coefficient of mirror 1. This condition must hold at all points in the plane $z = 0$, and so in this plane we must have $u_+(\boldsymbol{r}, \omega, t) = u_-(\boldsymbol{r}, \omega, t)$, that is that the positive- and negative-going waves must be in the same mode. We can therefore simplify eqn (7.1) to,

$$a_+(0,\omega) = a_-(0,\omega)r_1 e^{i\phi_1}. \tag{7.2}$$

Similarly, after propagating to mirror 2 and back, the right-going wave starting at $z = 0$ must be the same as the negative-going wave at $z = 0$:

$$a_-(0,\omega) = a_+(0,\omega)e^{i(\delta_{rt}-\phi_1)}\, r_2, \tag{7.3}$$

where δ_{rt} is the optical phase accumulated by the mode in propagating one complete round trip (including any phase shifts arising from the two mirrors), and r_2 and ϕ_2 are the modulus and phase respectively of the amplitude reflection coefficient of mirror 2. We can combine this result with eqn (7.2) to give,

$$a_+(0,\omega) = a_+(0,\omega)r_2 r_1 e^{i\delta_{rt}}. \tag{7.4}$$

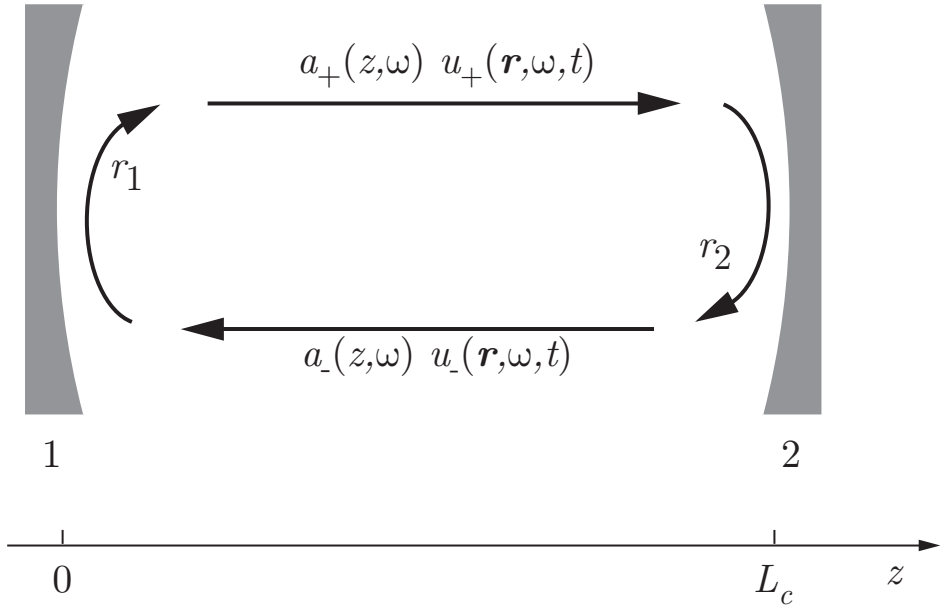

Figure 7.1: Cavity effects in a laser oscillator.

It must therefore be that under steady-state conditions,

$$r_2 r_1 \mathrm{e}^{\mathrm{i}\delta_{\mathrm{rt}}} = 1. \tag{7.5}$$

Equation (7.5) is complex and hence we can extract 2 conditions. The imaginary part of the right-hand side is zero, which means that δ_{rt} must equal an integer times π. Further, $r_1, r_2 > 0$ and hence $\exp(\mathrm{i}\delta_{\mathrm{rt}})$ must also be positive. Thus we conclude that eqn (7.5) can only be satisfied if

$$\delta_{\mathrm{rt}} = 2\pi p. \qquad p = 0, 1, 2, 3, + \ldots \tag{7.6}$$

Of course, (7.5) also requires $r_1 = r_2 = 1$ which would require perfect mirrors. The fact that in a real cavity $|r_1|, |r_2| < 1$ means that steady-state conditions can only be achieved if we introduce gain in to the cavity, as we discuss in the following section.

Let us consider the condition on δ_{rt} in more detail by way of a simple example. Suppose that the cavity is filled uniformly with material of refractive index n. Then, $\delta_{\mathrm{rt}} = 2kL_{\mathrm{c}}$ and hence we could write eqn (7.6) as

$$2k_p L_{\mathrm{c}} = 2\pi p \qquad p = 0, 1, 2, 3, + \ldots. \tag{7.7}$$

In terms of frequency (not angular) this condition becomes:

$$\nu_p = \frac{\mathrm{c}}{2nL_{\mathrm{c}}} p, \qquad \textbf{Longitudinal modes} \tag{7.8}$$

We see that only certain frequencies will oscillate, corresponding to the resonant frequencies or **longitudinal modes** of the optical cavity. The frequency spacing between adjacent longitudinal modes is[1],

$$\Delta\nu_{p,p-1} = \frac{\mathrm{c}}{2nL_{\mathrm{c}}}. \tag{7.9}$$

7.1.1 Insertion of gain into the cavity: The laser threshold condition

Now let us suppose that we place a gain medium of length L_g within the optical cavity. Now as radiation circulates around the cavity it will be amplified as it passes through the gain medium, and so may overcome the cavity losses.

[1] You should convince yourself that this is just the free-spectral range of the cavity when used as a Fabry-Perot etalon.

We wish to calculate a condition for the laser reaching the threshold for laser oscillation. Near threshold the intensity of the circulating radiation must be very small, so that the gain will be unsaturated, and the circulating radiation is amplified according to the unsaturated gain coefficient. Denoting the threshold value of the unsaturated gain coefficient by $\alpha_0^{\rm th}$, with the insertion of gain in the optical cavity eqn (7.3) becomes at threshold:

$$\begin{aligned} a_-(0,\omega) &= a_+(0,\omega)\exp\left[\frac{1}{2}\alpha_0^{\rm th}(\omega)L_g\right]\exp\left[-\frac{1}{2}\kappa(\omega)L_{\rm c}\right] \\ &\times\ r_2\exp\left[\frac{1}{2}\alpha_0^{\rm th}(\omega)L_g\right]\exp\left[-\frac{1}{2}\kappa(\omega)L_{\rm c}\right]\exp\left[{\rm i}(\delta_{\rm rt}-\phi_1)\right]. \end{aligned} \tag{7.10}$$

Here κ is an absorption coefficient, which is introduced to represent any (unwanted) losses within the cavity *in addition* to the losses at the cavity mirrors. For convenience we have assumed that these losses are distributed uniformly over the whole length, $L_{\rm c}$, of the cavity. Notice how, for example, the amplitude of the positive-going wave is amplified by a factor of $\exp\left[\frac{1}{2}\alpha_0^{\rm th}(\omega)L_g\right]$ — the factor of $\frac{1}{2}$ arises since we are calculating the growth of the *amplitude* of the radiation rather than its intensity. The same factor appears in the term representing absorption for the same reason.

Combining eqns (7.10) and (7.2) we have

$$r_2 r_1\exp\left[\alpha_0^{\rm th}(\omega)L_g\right]\exp\left[-\kappa(\omega)L_{\rm c}\right]\exp\left({\rm i}\delta_{\rm rt}\right)=1. \tag{7.11}$$

Following the argument above, we see that we must have $\exp({\rm i}\delta_{\rm rt})=1$, and hence the *frequency of the radiation must correspond to one of the cavity modes.*

Equating the real parts of both sides of eqn (7.11) gives,

$$r_1 r_2\exp[\alpha_0^{\rm th}(\omega_p)L_g]\exp[-\kappa(\omega_p)L_{\rm c}]=1, \tag{7.12}$$

where the subscript p reminds us that the frequency must correspond to a cavity mode. Taking the square-modulus of both sides we find the threshold condition for lasing in terms of the power reflectivities R_1 and R_2 of the cavity mirrors:

$$R_1R_2\exp[2\alpha_0^{\rm th}(\omega_p)L_g]\exp[-2\kappa(\omega_p)L_{\rm c}]=1. \qquad \textbf{Threshold condition} \tag{7.13}$$

This last result has a straightforward interpretation: if we imagine launching a beam of unit intensity from within the cavity, after one round-trip it would have an intensity equal to the left-hand side of eqn (7.13); if this is less than unity the beam will decay in intensity with each round-trip; if it is greater than unity, the beam will grow in intensity. Equation (7.13) therefore gives the condition for steady-state laser oscillation. It may be written in the alternative form,

$$2\alpha_0^{\rm th}(\omega_p)L_g=2\kappa(\omega_p)L_{\rm c}-\ln(R_1R_2). \quad \textbf{Threshold condition} \tag{7.14}$$

To summarize, laser oscillation can only occur if *for some cavity mode the unsaturated round-trip gain exceeds the round-trip loss.* The threshold condition determines — for a given laser cavity — a threshold value for the gain coefficient. In turn this defines, for a given laser transition, threshold values for the population inversion and the rate of pumping of the upper laser level.

7.2 Laser operation above threshold

In deriving the conditions required to reach laser oscillation we noted that under steady-state conditions the round-trip gain experienced by an oscillating cavity mode must be balanced by the round-trip loss. Of course, this must also be true if the laser is operating above threshold — that is, we are pumping the laser gain medium harder. However, in this case the gain experienced by the radiation circulating within the cavity will be *saturated*, at least to some extent, by the laser radiation circulating within the cavity. We will see that it is this saturation that reduces the round-trip gain so that it is in balance with the cavity losses.

Let us consider how a homogeneously-broadened laser system behaves as we gradually increase the pumping of the gain medium (by, for example, increasing the flashlamp voltage). As the pumping is increased from below the threshold value the population inversion N^* will increase until the small-signal gain for the

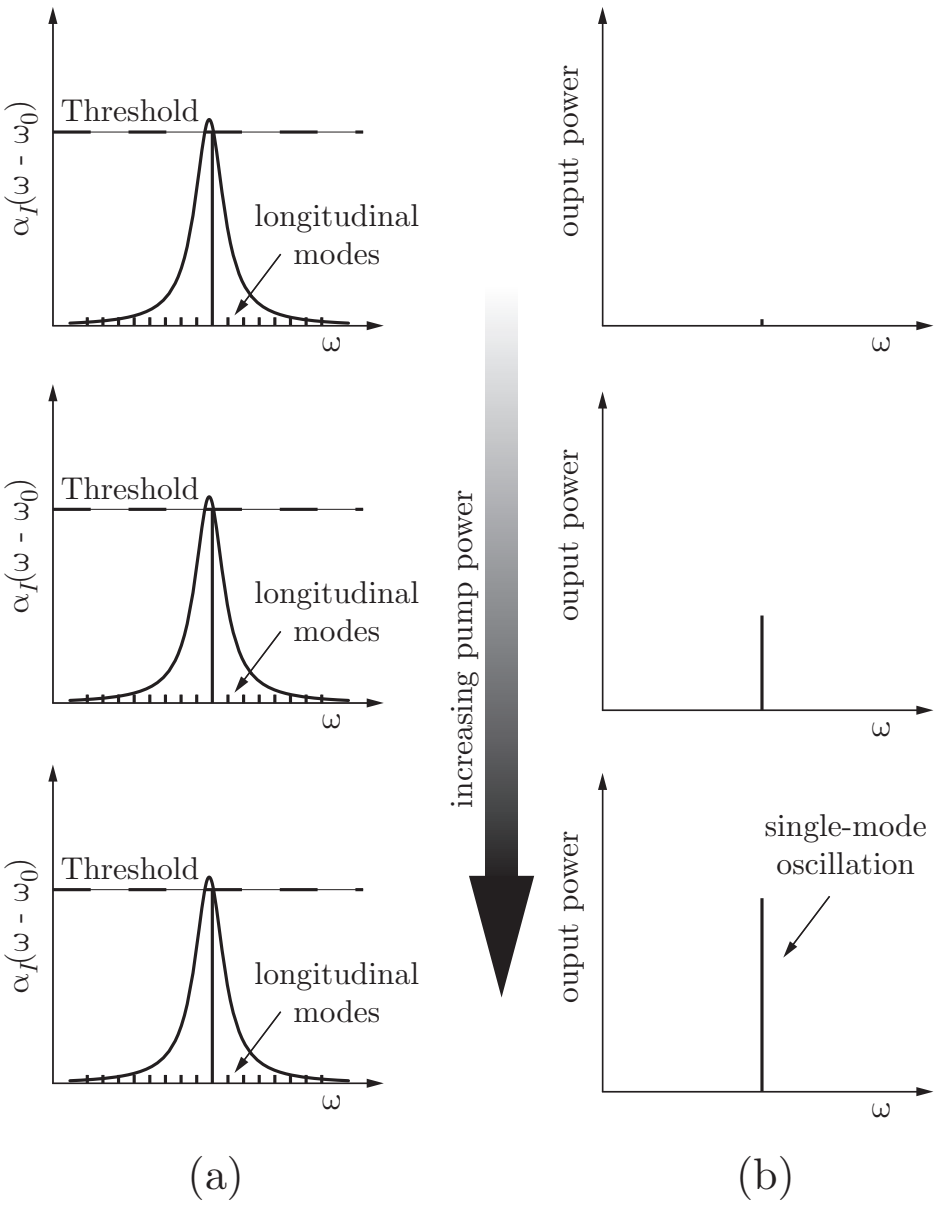

Figure 7.2: Schematic diagram showing, for a homogeneously-broadened laser transition, the effect of increasing the pump rate above threshold on: (a) the gain coefficient; (b) the intensity of the oscillating mode. Note that the gain curve does not change with increased pumping, as explained in the text.

mode closest to the line centre reaches the threshold value determined by the cavity losses. This will cause a very large (of order 10^{15}) increase in the energy density of the radiation field at the frequency of the oscillating mode.

What happens if the pumping is increased further? Perhaps surprisingly, neither the gain coefficient $\alpha_I(\omega)$, or the population inversion will increase. The reason is that in the steady-state, the round-trip gain must always be balanced by the round-trip loss.

How is this balance maintained? Whilst it is true that increasing the pumping rate R_2 will increase the rate at which the upper laser level is populated, this is accompanied by an increase in the intensity of the oscillating mode which increases the rate of depopulation of the upper laser level by stimulated emission. Thus, the increased radiation intensity acts to burn down the population inversion and *maintains it (and the gain coefficient) so that the round-trip gain equals the round-trip loss.* It is important to note that, since the gain medium is homogeneously-broadened,[2] the entire population inversion is burnt down to the threshold value so that the entire gain profile $\alpha(\omega)$ is locked at the threshold value so that $\alpha_I(\omega_p) = \alpha_0^{\rm th}(\omega_p)$.[3] This

[2]The behaviour is quite different for inhomogeneously-broadened gain media.

[3]This last statement is a slight simplification (which is perfectly adequate for the present purpose). If the intensity varies significantly from one end of the gain medium to the other, as would happen if the cavity losses were very high, we cannot talk about 'the' gain coefficient since the gain coefficient will depend on z. However, even in these more complicated situations it remains the case that saturation will burn the population down to the point that the round-trip gain is balanced by the

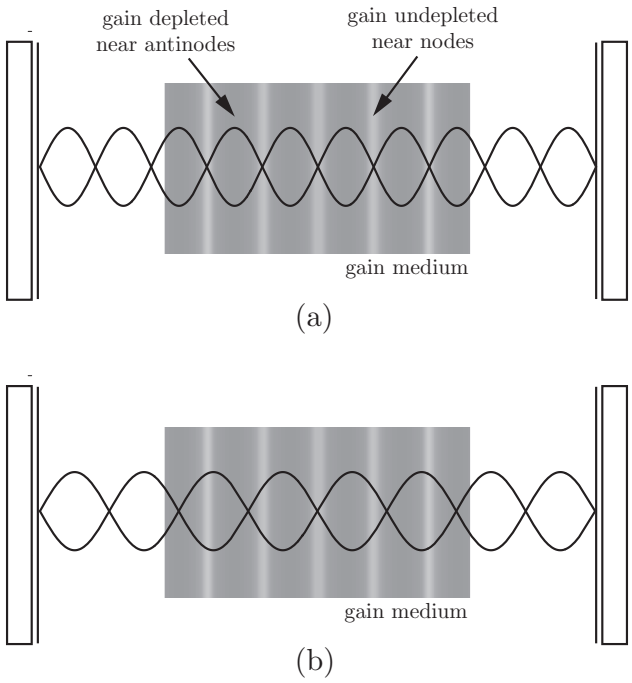

Figure 7.3: Spatial hole-burning in a homogeneously broadened steady-state laser oscillator. In (a) the standing wave of an oscillating mode causes the gain to be depleted where the intensity is high. However, the gain is unaffected near the nodes of the standing wave since the intensity in these regions is low. This can allow other cavity modes — which will have a different frequency and hence different locations for the nodes and antinodes in its standing wave pattern — to feed off the regions of unused gain, as shown in (b).

process is shown schematically in Figure 7.2.

7.2.1 Spatial hole-burning

It would seem from this argument that only one mode could ever be brought into oscillation in a homogeneously broadened laser. This is not always so, however. Within a laser cavity the oscillating mode forms a standing wave. Near the nodes of the standing wave the electric field is at all times small, and so the population inversion in this region will not be burnt down to the same extent as near the anti-nodes. Consequently a longitudinal mode at a slightly different frequency can establish itself by feeding on the high levels of the population inversion found at the nodes, as illustrated schematically in Fig. 7.3. This process is known as **spatial hole-burning**. Spatial hole-burning can be avoided by using a ring cavity[4] and restricting laser oscillation to one direction round the cavity, since then no standing wave is formed.

7.3 Frequency tuning

If the linewidth of the laser gain medium is sufficiently broad, such as in the Ti:sapphire laser discussed later, the wavelength of the laser output can be tuned. Tunable sources of this type are invaluable in a wide variety of scientific and industrial applications, such as spectroscopy, detection of atmospheric pollutants etc.

Diffraction gratings, birefringent filters, and prisms can all be used to tune the output wavelength; their role is simply to make the feedback of the laser cavity depend on wavelength. Fig. 7.4 shows a diffraction grating used at grazing-incidence to provide wavelength-dependent feedback. The grating is used at grazing incidence to increase the number of grating lines illuminated by the circulating laser beam, since the minimum resolvable frequency width of a grating is inversely proportional to the width of the illuminated part of the grating. The grating is usually blazed to minimize the losses for the selected wavelength. However, for very large angles of incidence (i.e./ close to grazing), blazed gratings can become lossy since the highest part of each grating groove shadows the subsequent groove. To overcome this, asymmetric prisms are often used to expand the size of the beam in one dimension, which helps increase the width of grating illuminated for a given angle of incidence.

round-trip loss.

[4] A laser cavity formed from three or more mirrors in which the path taken by the light forms a polygon of finite area.

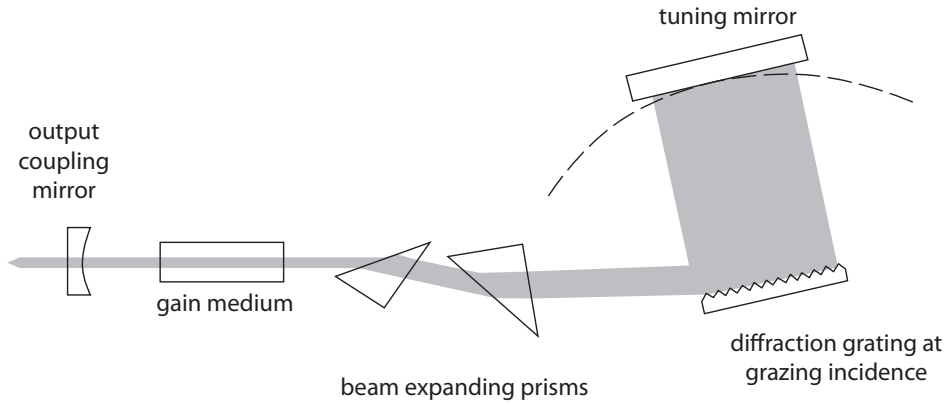

Figure 7.4: Wavelength tuning with a grazing-incidence diffraction grating.

Frequency tuning may also be obtained by one or more birefringent filters. At its simplest a birefringent filter is a plate of birefringent material with its optical axis in the plane of the plate. The normal to the plate is usually oriented at Brewster's angle with respect to the incident light in order to reduce reflection losses. The retardance introduced by the plate depends on the wavelength of light and on the angle between the optic axis and the direction of propagation within the plate. Those wavelengths for which the plate acts as a full-wave plate are transmitted with no change of polarization state and zero reflection losses. For other wavelengths the polarization state is changed and the transmission losses suffered at the rear surface of the plate, and at other polarization-sensitive elements (such as the laser rod), are finite. The filter may be tuned by rotating the plate about an axis parallel to its normal. In practice several such plates may be employed, with different free spectral ranges, so as to select a single wavelength.

Lecture 8

Solid-state lasers

8.1 Solid-state lasers

A very large number of scientifically and commercially important lasers operate with solid-state gain media. Solid-state lasers, as distinct from lasers operating in gases or liquids, are attractive since they can often be made to be rugged and compact, there are no gas or liquid bottles with their associated handling equipment, and there is no chemical hazard. Of course, solid-state lasers are restricted to operating in wavelength ranges with good transmission through solid materials (i.e. infrared to ultraviolet). In addition, the time-averaged output power that a solid-state laser can deliver is often limited by the need to remove waste heat from the gain medium so as to avoid thermal distortion or even melting.

For many solid-state lasers the active lasant species are impurity ions doped into an insulating crystalline or glassy solid. Figure 8.1 shows schematically the energy level diagram of the active laser ions in such a system.

The spectroscopy of an impurity ion doped into a solid host depends on the strength with which the ion interact with the surrounding ions. If this interaction is weak the energy levels of the ion will be similar to those of the free ion, although the levels will generally be broadened by interactions with lattice phonons. If the interaction with the surrounding ions is strong, the structure and labelling of the energy levels will be very different; furthermore, transitions in which both photons and phonons are emitted become possible, as discussed below.

The basic operation of a solid-state laser is as follows:

- The population inversion is achieved by optical pumping on broad **pump bands** $0 \rightarrow 3$. The broad nature of the pump bands reduces the difficulty of carefully matching the frequency of the pump light to that of the pump transition, and also allows pumping by broad-band sources such as flashlamps.
- Level 3 decays rapidly by non-radiative processes to populate a range of lower levels. The proportion of decays from level 3 that populate the upper laser level 2 is known as the **branching ratio** η_{branch}.
- If the pumping is sufficient to realize a population inversion, lasing occurs on the transition $2 \rightarrow 1$.
- If the lower laser level lies close to ($E_1 \ll k_{\text{B}}T$), or is, the ground state it will have a large thermal population. In this case there are essentially only 3 levels of importance, and the laser is classed as a **three-level laser**.
- In contrast, if the lower level is well above ($E_1 \gg k_{\text{B}}T$) the ground state, the laser is classed as a **four-level laser**. To avoid build-up of population in the lower laser level, known as **bottlenecking**, it is desirable for the lifetime of the lower level to be short.

8.2 The Nd:YAG laser

The most widely used laser based on doping of the active ion in an insulating solid is the Nd:YAG laser in which Nd^{3+} ions are doped into an Yttrium Aluminium Garnet (YAG) crystalline host.

A simplified energy level diagram for Nd^{3+} ions doped in YAG is shown in Fig. 8.2. The ground configuration of the Nd^{3+} ion comprises a Xe-like core plus three 4f electrons. The 4f orbitals are more compact than the 5s and 5p orbitals, which are also occupied. As such, the mean radius of the 4f orbitals is relatively small compared to the size of the Nd^{3+} ion and compared to the distance to the surrounding ions of the lattice. As a consequence the interaction of the Nd^{3+} ions with surrounding ions is relatively weak, and hence the energy levels are similar to those of the free ion.

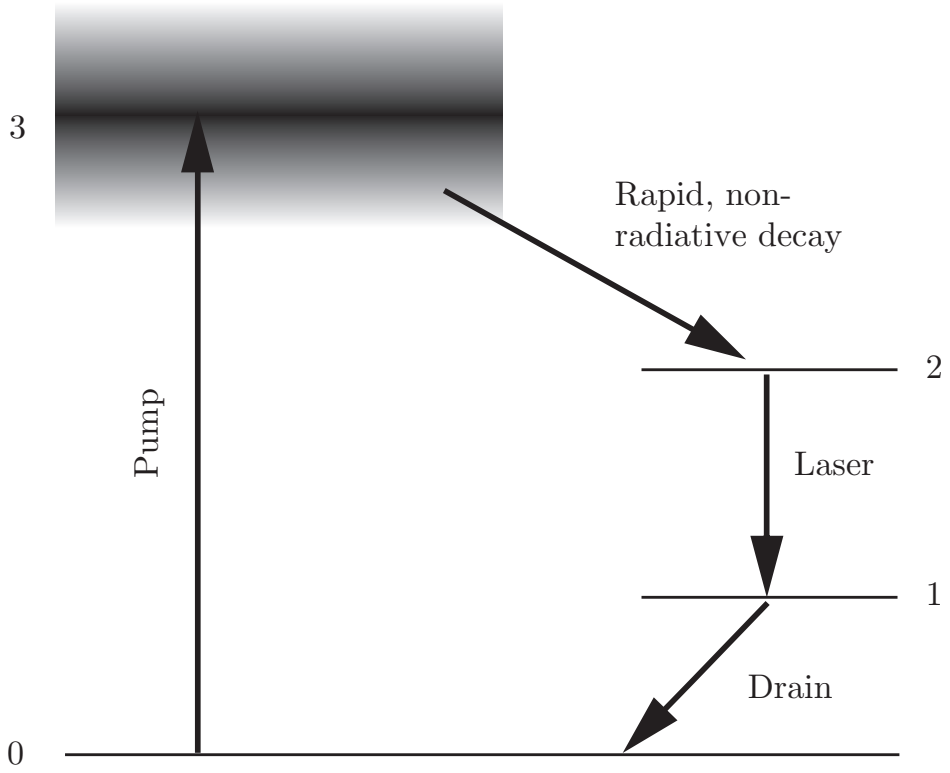

Figure 8.1: Schematic diagram of a general optically-pumped solid-state laser system.

All of the levels of interest to the Nd:YAG laser arise from the 4f configuration: this configuration is split into terms and levels by the residual electrostatic and spin-orbit interactions, with further small splitting arising from the weak interaction with the crystal field. The Nd^{3+} ions occupy equivalent sites in the YAG lattice, and hence the centre frequencies of the transitions are the same for all ions[1]. The laser lines are broadened by phonon interactions to a width of approximately 2×10^{11} Hz.

The laser pump bands occur at wavelengths of approximately 730 nm and 800 nm, and in fact this absorption bands cause the otherwise colourless YAG crystal to appear purple. Ions excited to these levels decay rapidly, and non-radiatively, with a lifetime of order 100 ns to the $^4F_{3/2}$ level at approximately 11 500 cm^{-1}. There is a significant energy gap from the $^4F_{3/2}$ level to the next lower level, and consequently the rate of non-radiative decay of the upper laser level is relatively slow. Instead the level decays predominantly by radiative emission to the ^4I levels, with a lifetime of 230 μs. The strongest transition is to the lower laser level, $^4I_{11/2}$, at approximately 2 000 cm^{-1}. The wavelength of the Nd:YAG laser is therefore[2] 1064 nm. We should also note that the $^4F_{3/2}$ and $^4I_{11/2}$ levels are split into 2 and 6 levels respectively, and in fact lasing occurs on two, closely-spaced transitions.

Since the lower laser level lies well above the ground state, its thermal population will be small relative to that of the ground state (a fraction of approximately $\exp(-2000/210) \approx 10^{-4}$). Further, the lower laser level undergoes rapid (ns) non-radiative decay to the ground state, and consequently the population of the lower laser level is small even during lasing. As such the Nd:YAG laser is a good example of a four-level laser. The favourable lifetime ratio, and the selective pumping ensure that it is relatively easy to achieve a population inversion in this system.

8.2.1 Threshold for pulsed operation

Figure 8.3 shows an idealized energy level diagram for calculation of the threshold pump energy for laser oscillation. Assuming that the cavity losses are small, the threshold condition for laser oscillation may be written,

[1]This is not the case for Nd^{3+} ions doped into glass, and consequently Nd:Glass lasers are inhomogeneously-broadened and have a much larger linewidth.

[2]The use of non-linear crystals to frequency double, triple, or even quadruple the fundamental of the Nd:YAG laser to wavelengths of 532 nm, 354 nm, and 266 nm is very common in applications of this laser.

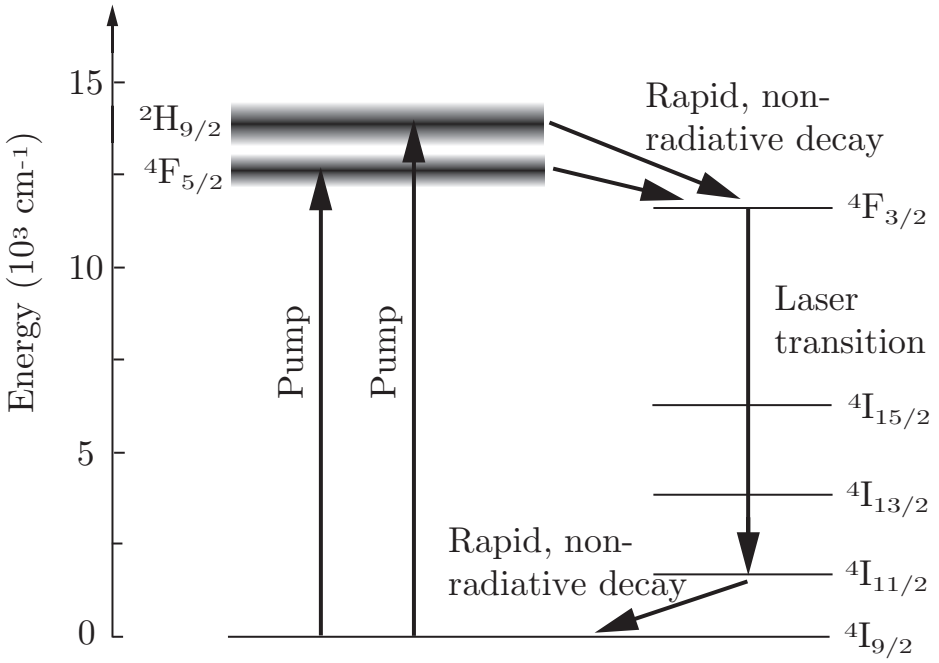

Figure 8.2: Energy levels of importance to the Nd:YAG laser.

$$2\alpha_0 L_{\rm g} = \delta_{\rm loss} + T_2 \tag{8.1}$$

$$2\sigma_{21} N^*_{\rm thresh} L_{\rm g} = \delta_{\rm loss} + T_2, \tag{8.2}$$

where $N^*_{\rm thresh}$ is the threshold population inversion. Taking the losses on the right-hand side to be (say) 10%, and assuming a typical length of laser rod of $L_{\rm g} = 50$ mm and a gain cross-section of 6×10^{-19} cm^2, we find $N^*_{\rm thresh} \approx 1.6 \times 10^{16}$ cm^{-3}.

Now, for a four-level laser $N_1 \approx 0$, and hence we have,

$$N_2^{\rm thresh} = N^*_{\rm thresh}. \qquad \textbf{Threshold condition for YAG} \tag{8.3}$$

Having calculated the threshold upper level population density, it is straightforward to estimate the energy required to do this. Taking the pump laser radiation to have a wavelength of $\lambda_{\rm p} \approx 750$ nm, the energy required to raise each ion to the upper laser level is $hc/\lambda \approx 1.65$ eV. The threshold pump energy is therefore,

$$E_{\rm abs}^{\rm thresh} = N_2^{\rm thresh} \left(\pi a^2 L_{\rm g}\right) \frac{hc}{\lambda_{\rm p}}, \tag{8.4}$$

where a and $L_{\rm g}$ are the radius and length of the laser rod. Taking $a = 2$ mm, $L_{\rm g} = 20$ mm, we find $E_{\rm abs}^{\rm thresh} \approx 1.8$ mJ.

This last figure, however, is the energy that must be absorbed by the laser rod. The electrical energy supplied must be larger by a factor of about 60 as follows:

×2 To achieve uniform pumping within the laser rod the doping and diameter must be such that only approximately 50% of the pump photons are absorbed. If the Cr^{3+} concentration is higher, or the rod diameter larger, population inversion is only achieved near the surface of the rod;

×8 Only approximately 12% of the output of the flashlamp will lie in the pump bands;

×2 Only about 50% of the pump light is geometrically coupled into the rod;

×1.7 Only 60% of the electrical energy is converted into light.

In our numerical example, the threshold pump energy that must be supplied to the flashlamps is therefore of order 100 mJ.

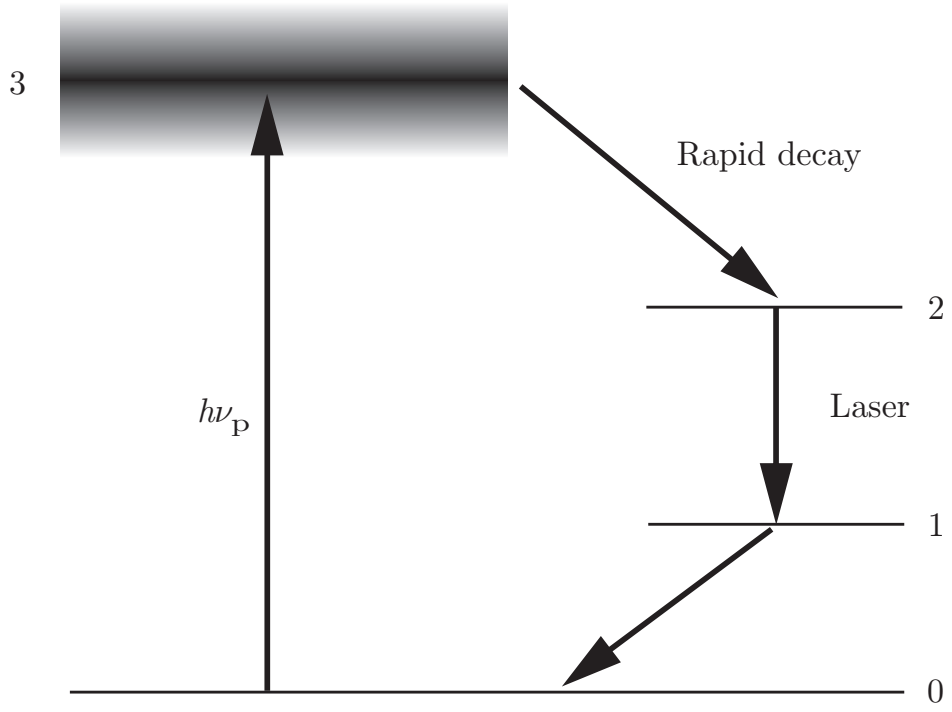

Figure 8.3: Simplified energy level diagram for calculation of the threshold pump energy in a four-level laser.

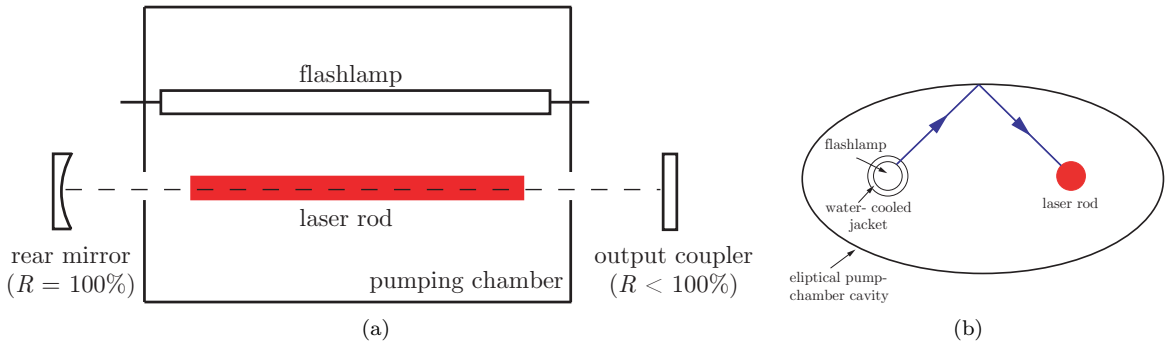

Figure 8.4: Schematic diagram showing: (a) the general layout of a flashlamp-pumped solid-state laser; (b) use of an elliptical pumping chamber to increase the efficiency with which flashlamp radiation is coupled into the laser rod.

8.2.2 Threshold for c.w. operation

In order to calculate the pump power required to achieve continuous operation of the laser, we note that the upper level population density will decay spontaneously at a rate N_2/τ_2. Consequently the threshold pump power for c.w. operation is simply the threshold pump energy divided by the upper laser level lifetime. With $\tau_2 \approx 230\,\mu$s we find a threshold electrical pump power of order 400 W. This can be achieved relatively easily.

8.2.3 Practical devices

Figure 8.4 shows the general layout employed for flashlamp-pumping a solid-state laser. A key component is the pumping chamber used to couple light from the flashlamp (or lamps) into the laser rod. A wide variety of geometries for the pump chamber have been developed, including double-elliptical cavities for coupling light from two flashlamps into a single laser rod, and cavities employing highly-reflecting diffusive surfaces which can give very uniform illumination of the active medium. The flashlamp can also be coiled around the laser rod which avoids the need for a cavity for the pump light but is less efficient.

The Nd:YAG laser can also be optically pumped with the radiation from high-power semiconductor, or 'diode', lasers and in particular GaAlAs lasers operating close to the 800 nm pump band of Nd:YAG. Diode lasers of this type are very efficient, their electrical efficiency can reach 50%. Pumping with diode lasers has several advantages over flashlamp pumping: all of the output lies within the pump band of the Nd:YAG

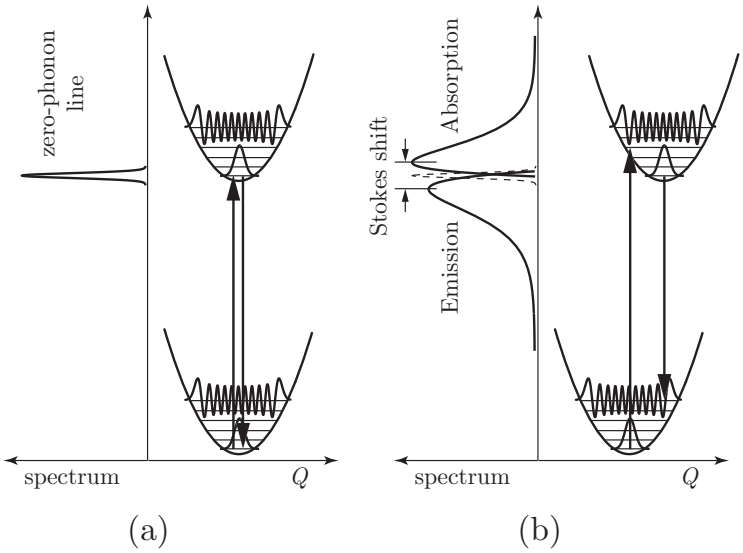

Figure 8.5: Transitions between electronic levels: (a) when the equilibrium configuration co-ordinate is essentially the same for the upper and lower electronic levels; (b) when the equilibrium configuration coordinates are different for the two levels, causing the potential curves to be displaced. Vibrational wave functions are illustrated schematically for the lowest vibrational level and an excited vibrational level. In (b) the position of the zero-phonon line is shown by the dotted curve.

laser, improving efficiency and reducing thermal load on the system; the output is unidirectional and so easier to couple in to the laser rod. As a result the overall electrical efficiency of diode-pumped Nd:YAG (and other diode-pumped solid-state) lasers can exceed 1%.

8.3 Trivalent iron-group lasers

The ground-state configuration of the trivalent ions of the iron-group is [Ar]3d^n. Since the 3d orbitals are larger than the 4f orbitals of the trivalent rare earths, and the radius of the ionic size is smaller, the interaction with the crystal field is much stronger — indeed it can be stronger than either the residual electrostatic or spin-orbit interactions. As such the energy levels of the trivalent iron-group ions is very different from the corresponding free ion.

8.3.1 Configuration coordinate picture

Since the interaction with the surrounding ions is strong, the energy levels of the active ion depend strongly on the positions of the surrounding ions of the lattice. To simplify the multi-dimensional problem we imagine parameterizing the distance between the active and surrounding ions with a single parameter: the configuration coordinate Q. We can think of this as representing the average nearest-neighbour distance.

In principle the energy levels of this system can be solved using the same approach used to find the energies of diatomic molecules. The Schrödinger equation for the system can be written as,

$$\left[\hat{T}_\mathrm{n} + \hat{T}_\mathrm{e} + V(Q, \boldsymbol{R})\right] \Psi(Q, \boldsymbol{r}) = E\Psi(Q, \boldsymbol{r}), \tag{8.5}$$

where $\hat{T}_\mathrm{n}$ is the kinetic energy operator of the active and surrounding ions, $\hat{T}_\mathrm{e}$ the kinetic operator of the electrons of the active ion, $V(Q, \boldsymbol{R})$ the potential energy arising from the electrostatic interactions between electrons and ions. By making the Born-Oppenheimer approximation, we find that the active ion moves in a potential well, $E(Q)$, which is the energy eigenvalue found by solving the Schrödinger equation for a fixed value of Q. This configuration co-ordinate picture can be used to explain the main features of the spectroscopy of ions which interact strongly with the surrounding ions.

8.3.2 Zero-phonon and vibronic transitions

Two types of transition occur within the configuration co-ordinate, depending on whether or not the equilibrium configuration co-ordinate, Q_0, is different for the upper and lower levels of the transition, as illustrated in 8.5(b).

Just as we found for diatomic molecules, the strength of the transition is proportional to the square of the overlap integral of the vibrational wave functions of the upper and lower level.

Suppose that the lower electronic level corresponds to the electronic ground-state, and let us consider optical excitation to the upper electronic level. The vibrational wave functions for the lowest vibrational level generally resemble a Gaussian curve, whilst those of high-lying levels are strongly peaked near the classical turning points. Absorption from the lower electronic level will be dominated by transitions from the lowest vibrational level, since this will have by far the largest thermal population.

If Q_0 is similar for the upper and lower levels, the strongest absorption will therefore be to the lowest vibrational level of the upper electronic level, as shown in 8.5(a), since the overlap integral for these two vibrational wave functions will be large. The overlap integral will be comparatively small for transitions to high-lying vibrational levels since the vibrational wave function of such levels show rapid oscillations and are only large near the classical turning points, where the amplitude of the wave function of the lowest vibrational level of the ground state is small. In any case, excitation to excited vibrational levels of the upper electronic level will be followed by extremely rapid de-excitation to the lowest vibrational level by phonon de-excitation. The emission spectrum will therefore be dominated by emission from the lowest vibrational level of the upper electronic level. Just as for the absorption spectrum, and for the same reason, the emission will be dominated by transitions to the lowest vibrational level of the electronic ground-state. In other words, when the equilibrium co-ordinates of the upper and lower electronic levels are similar the absorption and emission spectra are dominated by transitions from $v'' = 0$ to $v' = 0$, i.e. no change of vibrational quantum number, or equivalently, no emission or absorption of lattice phonons. Transitions of this type are known as **zero-phonon transitions**.

Very different behaviour occurs if the equilibrium configuration co-ordinates are different in the upper and lower levels, as shown in 8.5(b) . Now absorption from the lowest vibrational level of the ground electronic state is distributed over many vibrational levels of the upper electronic level, leading to absorption extending to higher frequencies than that of the zero-phonon line. Absorption at frequencies above that of the zero-phonon line corresponds to electronic excitation accompanied by excitation of lattice vibrations, or, equivalently, emission of phonons. Following absorption, ions in excited vibrational levels of the upper electronic level will undergo rapid phonon de-excitation to the lowest-lying vibrational level. Just as for the absorption, emission will then occur to a wide range of vibrational levels of the ground electronic state, producing a broad emission spectrum shifted to frequencies below that of the zero-phonon line. The absorption and emission spectra are widely separated, the separation in frequency between the peaks of the two spectra being known as the Stokes shift. Hence, transitions between electronic levels with different values of Q_0 are broad-band; they are known as **vibronic transitions**.

8.4 The ruby laser

In 1960 Maiman demonstrated laser oscillation in the optical region of the spectrum for the first time, using as the active medium a crystal of ruby. The active ion in ruby is Cr^{3+} doped at a level of around 0.05% by weight into sapphire (Al_2O_3).

The energy levels of interest to the ruby laser are shown schematically in Fig. 8.6. In ruby the Cr^{3+} ion has broad, vibronic absorption bands corresponding to excitation to the $^4T_1$ and $^4T_2$ levels (in this notation the superscript is equal to $2S+1$, where S is the total spin quantum number, but the letter 'T' is *not* related to the total orbital angular momentum, and instead indicates the symmetry of the wave functions).[3] These pump bands lie at approximately 24×10^3 and 18×10^3 cm^{-1} above the $^4A_2$ ground state. These absorption bands in the green and violet part of the visible spectrum cause a ruby laser rod to appear pink.[4]

Non-radiative relaxation of the ^4T levels to the nearby ^2E levels is very fast ($\tau \approx 50$ ns), and more probable than radiative decay back to the ground state. Optical pumping on the $^4T \leftarrow {}^4A_2$ pump bands therefore results in efficient transfer of population from the ground state to the upper laser levels.

The upper laser level, the ^2E level, has a similar configuration co-ordinate to the ground-state. Hence transitions to the ground state occur on a narrow, zero-phonon transition.

The upper laser levels decay predominantly by emission of radiation on transitions to the ground state. However, the radiative decay is forbidden by the electric dipole selection rules since: (i) the spin changes (from $S = 3/2$ to $S = 1/2$); (ii) there is no change of parity, since the electron configuration does not change. As a consequence the lifetime of the upper levels is long ($\tau_2 \approx 3$ ms). The long lifetime of the upper level means that it can act as a 'storage' level, which helps the formation of a population inversion.

The upper laser level is split into two levels separated by 29 cm^{-1}. The relative populations of these two levels is essentially thermalized by non-radiative transitions, and since $k_B T \approx 200$ cm^{-1} at room temperature the population of the higher of these levels is $\exp(-29/210) \approx 87\%$ of that of the lower of the levels. Laser

[3] In older notation, used in many laser textbooks, these levels are labelled $^4F_1$ and $^4F_2$.

[4] Ruby gemstones contain a much higher concentration of Cr^{3+}, nearer 1%, and consequently are a rich red colour.

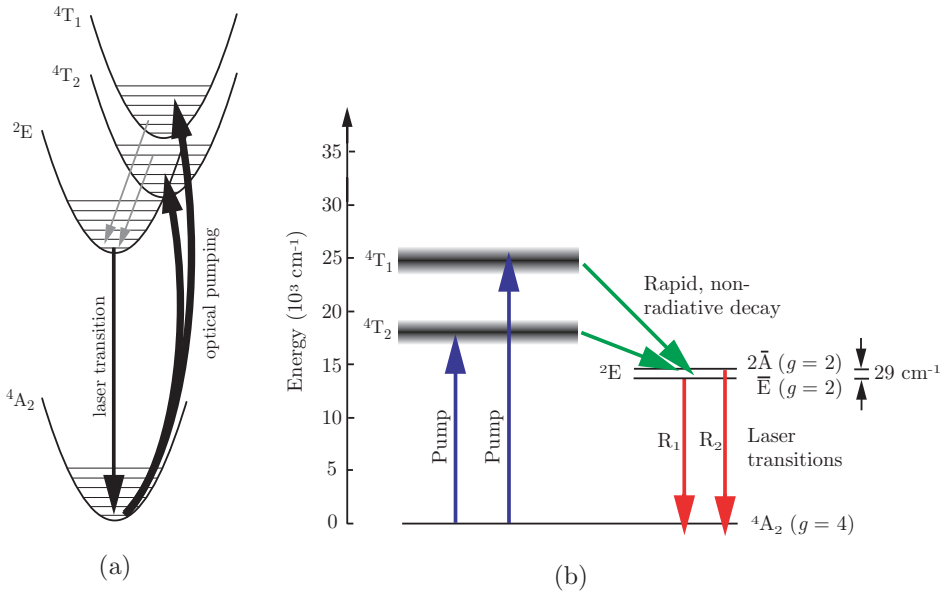

Figure 8.6: Energy levels of importance to the ruby laser. (a) configuration co-ordinate diagram; (b) simplified energy level diagram. The energy separation of the ^2E levels is exaggerated for clarity.

oscillation therefore usually occurs from the lower of the two levels (on the R_1 transition) at 694 nm, although lasing from the higher level (on the R_2 transition) at 693 nm is possible with a frequency-selective cavity.

We see that the energy level structure of ruby has some desirable features for a laser system: a strong, selective mechanism for pumping the upper laser level; a relatively long upper level lifetime which helps the population inversion build-up. The major drawback, however, is that the lower laser level is the ground state! As such it will have a very large, non-decaying population. The only way that lasing can occur in ruby is if a large proportion (essentially half) of the ground state population can be transferred to the upper laser levels. It is interesting to estimate the pump energy required to do this.

8.4.1 Threshold for pulsed operation

Figure 8.7 shows a simplified energy level diagram for calculating the pump energy to reach the threshold for laser oscillation in ruby. Note that for simplicity we will treat the two upper laser levels as a single level with a degeneracy $g_2 = 4$, equal to that of the ground state.

Assuming that the cavity losses are small the threshold condition for laser oscillation may be written,

$$2\sigma_{21} N^*_{\text{thresh}} L_{\text{g}} = \delta_{\text{loss}} + T_2, \tag{8.6}$$

where N^*_{thresh} is the threshold population inversion.

The ruby laser is clearly a three-level system, and since level 3 decays so rapidly to the upper laser level we have $N_3 \approx 0$. We may then write,

$$N_{\text{T}} = N_2 + N_1 \tag{8.7}$$

$$N^*_{\text{thresh}} = N_2^{\text{thresh}} - N_1^{\text{thresh}}, \tag{8.8}$$

where N_{T} is the total Cr^{3+} ion density, and N_2^{thresh} and N_1^{thresh} the upper and lower population densities at threshold. We then find, straightforwardly that,

$$N_2^{\text{thresh}} = \frac{N_{\text{T}} + N^*_{\text{thresh}}}{2}. \tag{8.9}$$

In practice the threshold population inversion density required for lasing will be tiny compared to the total ion density, and hence

$$N_2^{\text{thresh}} = \frac{N_{\text{T}}}{2}. \quad \textbf{Threshold condition for ruby} \tag{8.10}$$

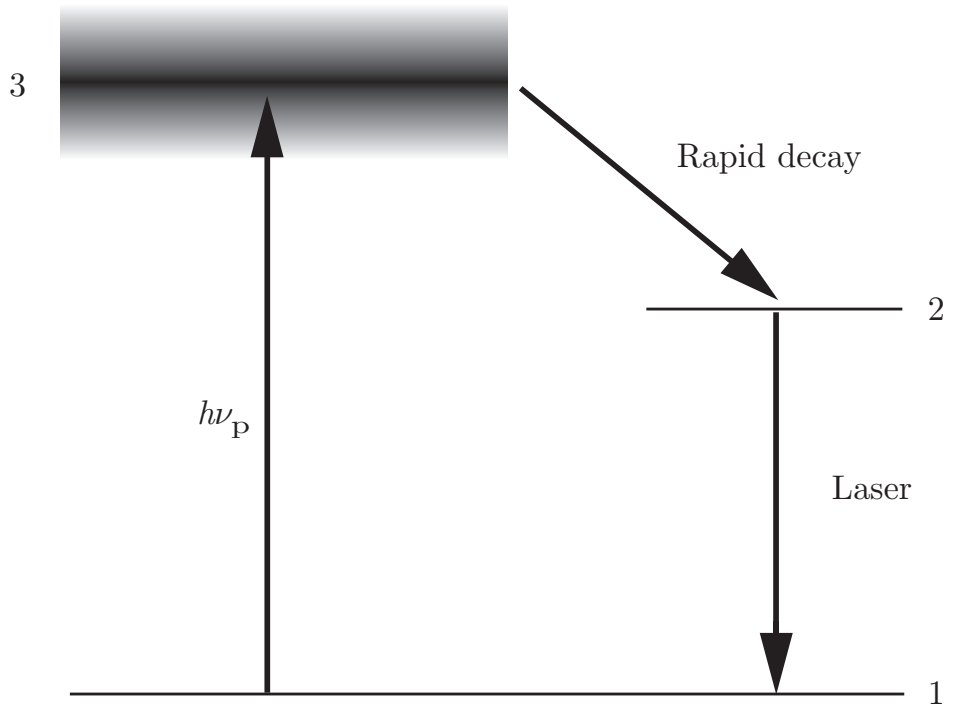

Figure 8.7: Simplified energy level diagram for calculation of the threshold pump energy in a three-level laser.

In other words, as hinted above, the main impediment to laser oscillation is the huge population density in the ground state. Once the ground state has been sufficiently depleted to equalize the populations in the upper and lower laser levels, the extra inversion require to overcome the cavity losses is relatively small.

Having calculated the threshold upper level population density, we use the same approach we employed for the Nd:YAG laser to estimate the energy required to achieve this population density:

$$E_{\rm abs}^{\rm thresh} = \frac{N_{\rm T}}{2}\pi a^2 L_{\rm g}\frac{hc}{\lambda_{\rm p}}, \tag{8.11}$$

where a and $L_{\rm g}$ are the radius and length of the laser rod. Taking $\lambda_{\rm p} \approx 500$ nm, $a = 5$ mm, $L_{\rm g} = 20$ mm, and $N_{\rm T} = 2 \times 10^{19}$ cm^{-3}, we find $E_{\rm abs}^{\rm thresh} \approx 6$ J.

As before, the electrical energy supplied must be larger by a factor of about 60, and hence the threshold pump energy that must be supplied to the flashlamps is of order 360 J.

8.4.2 Threshold for c.w. operation

As before the threshold pump power for c.w. operation is by dividing the threshold energy by the upper laser level lifetime. With $\tau_2 \approx 3$ ms we find a threshold electrical pump power of order 100 kW! The required pump power can be decreased by reducing the volume of the laser rod, but continuous operation of the ruby laser is still technically very difficult and because of this c.w. operation is of little practical importance.

8.4.3 Practical devices

The construction of ruby lasers is similar to that of Nd:YAG discussed above. Figure 8.8 shows the detail of one design of ruby laser. Note that in this design pump chamber is ellipsoidal, rather than the cylinder of elliptical cross-section shown in Fig 8.4. Notice also that the laser cavity is formed by coating the two ends of the ruby rod with silver to provide essentially 100 % reflection from the left-hand end of the rod, and partial transmission through the right-hand end.

8.5 The Ti:sapphire laser

The Ti:sapphire laser is an example of a laser operating on a vibronic transition. As such the linewidth of the laser transition is very broad, approximately 100 THz — the largest of any laser. The large bandwidth

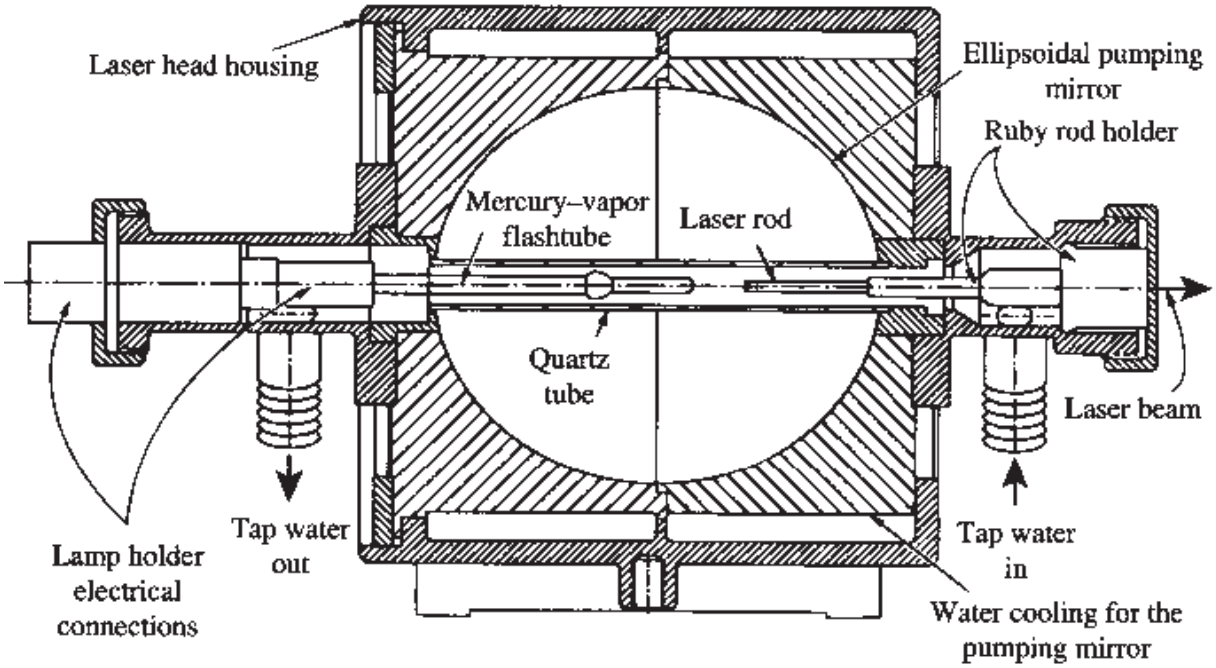

Figure 8.8: Schematic diagram of the construction of a ruby laser.

enables the wavelength of the laser to be tuned between approximately 700 nm and 1000 nm, making it an invaluable tool in a wide variety of scientific disciplines. The large bandwidth also means that Ti:sapphire can generate and amplify very short laser pules: oscillators can generate pulses as short as 5 fs, which is only a few optical cycles (generating pulses this short is technically difficult, but generating 30 fs pulses with a Ti:sapphire laser is routine).

The Ti^{3+} ion has only a single 3d electron outside a closed core, and hence has a very simple system of energy levels, as shown in Fig. 8.9(a). Absorption on the strong, vibronic $^2E \leftarrow {}^2T_2$ transitions to excited vibrational levels of the ^2E level with wavelengths between 630 nm and 400 nm. The excited ions then decay by rapid vibrational relaxation to the lowest vibrational level of the ^2E level, which forms the upper laser level. Ions in this level decay radiatively to excited vibrational levels of the ground electronic state with a lifetime of 3.2 μs. As should be clear, the Ti:sapphire laser is a four-level laser.

Although the bandwidth is very large, the large Einstein A-coefficient for the laser transition ensures that the cross-section is relatively high: approximately 3×10^{-19} cm^2.

8.5.1 Practical implementation

A major difference between Ti:sapphire and the ruby and Nd:YAG lasers is the short fluorescence lifetime of the upper laser level. Flashlamp pumping is therefore not usually very efficient owing to the much longer duration of the flashlamp pulse. Instead, laser pumping is usually used, the most commonly employed pump lasers being frequency-doubled Nd lasers (such as Nd:YAG).

Figure 8.9(b) shows the construction of a simple Ti:sapphire laser oscillator. The Ti:sapphire laser rod is 2 - 10 mm long, with end faces cut at Brewster's angle so as to eliminate reflection losses for one polarization. The z-folded cavity compensates for astigmatism. This arises because it is necessary to focus the pump radiation to a small cross-sectional area in order to achieve sufficient population inversion. The design of the optical cavity design must therefore be such that the transverse modes are also brought to a focus at the Ti:sapphire crystal. However, the Brewster-cut faces of the crystal introduce astigmatism to the intra-cavity beam — i.e. the divergence of the beam becomes different in the horizontal and vertical planes. In the cavity shown in Fig. 8.9(b) this is corrected by the two concave mirrors used away from normal incidence, which introduce astigmatism of the opposite sign to that caused by refraction at the laser rod.

Continuously-tunable c.w. Ti:sapphire lasers may be tuned between approximately 700 nm and 1000 nm, with output powers of 1 - 2 Watts. Wavelength tuning may be accomplished by a variety of techniques. In the design illustrated in Figure 8.9(b), tuning is achieved by adjusting a birefringent filter. In order to reduce losses, the filter can be mounted at Brewster's angle, and tuning achieved by rotating the filter about an axis parallel to its normal. Other techniques may, such as prisms or gratings, be employed for selecting

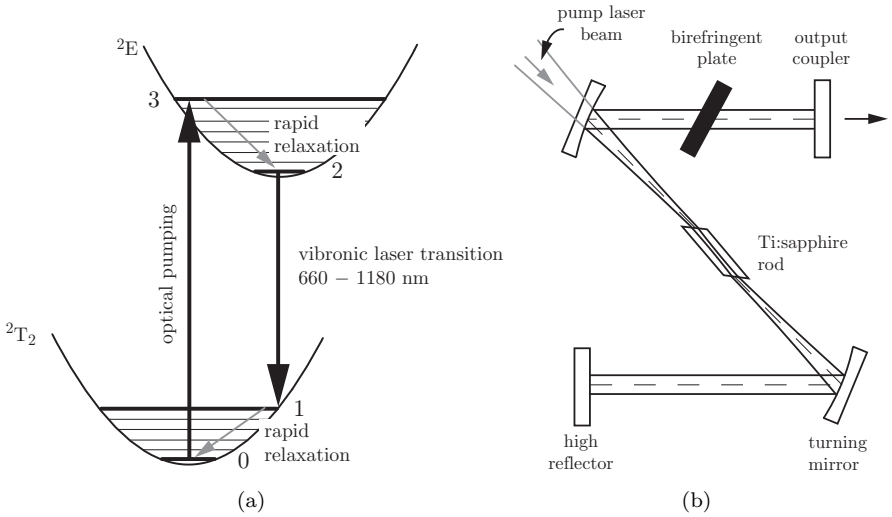

Figure 8.9: The Ti:sapphire laser. (a) Simplified energy level diagram. (b) Design of a tunable Ti:sapphire laser oscillator.

the output wavelength. For the oscillator shown in Fig. 8.9(b) the linewidth of the laser output is typically about 40 GHz; this may be reduced to better than 1 GHz by employing an intra-cavity etalon.